AN ELECTROSTATIC MODEL FOR THE METAL BINDING PROPERTIES OF HUMIC SUBSTANCES

by

Bettina Margrit Bartschat

S.B. in Chemistry, Massachusetts Institute of Technology
(1989)

SUBMITTED TO THE DEPARTMENT OF CIVIL ENGINEERING IN PARTIAL FULFILLMENT OF THE REQUIREMENTS FOR THE DEGREE OF

MASTER OF SCIENCE IN CIVIL ENGINEERING

at the

MASSACHUSETTS INSTITUTE OF TECHNOLOGY

August 1990

Signature of Author _____
Department of Civil Engineering
August 21, 1990

Certified by _____
Professor François M. M. Morel
Thesis Supervisor

Accepted by _____
Professor Ole S. Madsen
Chairman, Department Graduate Committee

AN ELECTROSTATIC MODEL FOR THE METAL BINDING PROPERTIES OF HUMIC SUBSTANCES

by

Bettina Margrit Banschat

Submitted to the Department of Civil Engineering on August 21, 1990 in partial fulfillment of the requirements for the degree of Master of Science in Civil Engineering.

Abstract

An oligo-electrolyte model of humic substances is developed to explain ionic strength effects on copper and hydrogen ion titrations. After discussing the relevance of various polyelectrolyte models to humic substances, two models are chosen in which the molecules are approximated by either ion-penetrable or impenetrable spheres. The electrostatic effect is calculated using numerical solutions of the appropriate non-linear Poisson-Boltzmann equations. The models are shown to converge on Debye-Hückel behavior when the molecular size is small, and on either Donnan or Gouy-Chapman behavior in the limit of large molecular size, depending on whether a penetrable or impenetrable geometry is used. A simple model, containing two copper binding sites and an additional acidic site, and two size classes of impenetrable spheres, is shown to be successful at explaining the ionic strength effects on cupric ion and pH titrations of fulvic acid.

Thesis Supervisor: Professor François M. M. Morel.
Title: Professor of Civil Engineering

The Buddha...resides quite as comfortably in the circuits of a digital computer or the gears of a cycle transmission as he does at the top of a mountain or in the petals of a flower.

Robert Pirsig, *Zen and the Art of Motorcycle Maintenance*

Acknowledgements

This is probably the most important page of my thesis. It is the only page that most people will ever read, and it gives me a chance to reflect on six years of MIT and Parson's Lab. I feel a bit like a newly hatched sea turtle, eagerly rushing off to some unknown fate in a mysterious ocean (but never forgetting where she was born).

Gifted teachers have contributed to the hatching of this scientist:

My father taught me early on to wonder and to ask questions of nature; my mother taught me compassion.

Penny Chisholm took me under her wings when I was a freshman, and introduced me to a field called oceanography; she has provided guidance and encouragement ever since.

François Morel, my advisor and mentor, taught me to take a question and make it mine, to grapple with it whenever it demanded (whether at seven in the morning or during a late afternoon swim), and to never be satisfied with half-answers. I thank him for the joy and the challenge I've found in our work.

Thanks are also due to many friends at Parson's Lab and Epsilon Theta. I shall name only a few: Pat and Sheila, the miracle workers of the third floor; Nalin, Hari, Cheo, Ede, and Rich, officemates and almost officemates, and patient sources of mathematical advice (No, Hari, it's not linear...); Sarah and Steve, the Experimentalists; Christina, word processing wizard and philosopher in her spare time; Corbin, Dianne, Dirk, Donald, Elaine, Linnea, and Topher, kindred spirits of the kind you recognize immediately and hang onto for the rest of your life; and Martin, *der Geduldige, er wartet schon in der anderen Welt jenseits des Ozeans.*

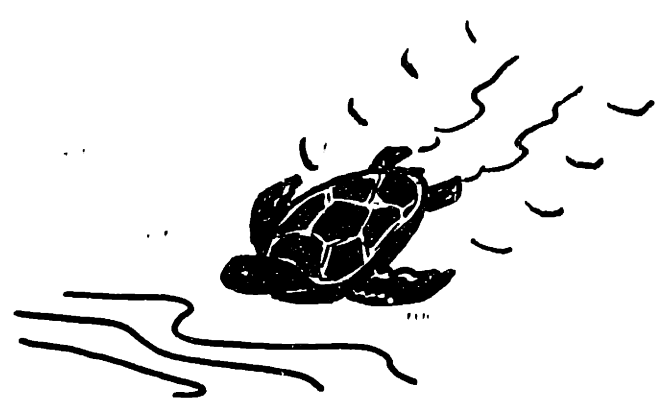

Table of Contents

Introduction

Humic substances abound in natural waters and may have significant effects on metal speciation and mobility, especially in waters with high levels of dissolved organic carbon (DOC). At present, our ability to predict these effects using equilibrium models are quite limited. The interactions between humic substances and metal ions are not well-described by a set of equilibrium constants; "constants" relevant for one set of conditions may fail completely for another.

These so-called "conditional constants" have been used by many workers as a convenient method of describing data sets of metal binding by humic substances (for example Buffle *et al.* 1977, Mantoura and Riley 1975, Sunda and Hanson 1979). Usually two or three discrete binding sites are required to fit a given titration. Unfortunately, such constants cannot possibly be of use in predicting natural water speciation, since pH, ionic strength, and the presence of competing metals have all been shown to affect their value (pH: Sunda and Hanson 1979, ionic stength: Cabaniss 1986, Cd^{2+} effect on Cu^{2+} binding: Fish 1984); finding conditional constants for every possible set of conditions is a daunting task. A better approach is to wonder what affects these "constants". If we can determine the chemical reasons for the changes in binding strength under different conditions, we may be able to gain some ability to extrapolate from one set of conditions to another.

One often-stated possibility is that the humic substances' heterogeneity is the problem. After all, if no two humic acid molecules look exactly the same, then every binding site on every molecule should have a different binding constant. Instead of assuming the presence of a small number of individual binding sites to find conditional constants, some researchers have taken this heterogeneity into account by using a more statistical approach, using for example a Gaussian distribution of binding sites

around a mean log K or equilibrium constant (Perdue and Lytle,1983). This approach may be more pleasing conceptually, but the end result is similar to that of the discrete site model: a given titration data set can be described with a smaller number of fitting parameters, but extrapolation is still not possible.

A more important consideration regarding heterogeneity is that a different binding site may dominate the binding under different conditions. For example, proton competition may make the site which dominates at high pH's completely insignificant at low pH's. Cabaniss and Shuman (1988a) used this idea to simultaneously fit a series of copper-fulvate titrations carried out at different pH's, ionic strengths, and total DOC levels, using five discrete ligands of varying "protonicities" (a term referring to the number of protons exchanged when a site binds to a Cu^{2+} ion). All but the large ionic strength effects are adequately described by this model, although extrapolation to pH's outside of the range of calibration did not yield satisfying results. This is not surprising, since one would expect the protonicities of the copper binding sites to vary with pH as the sites deprotonate, an effect not included in the model. Another work by Cabaniss and Shuman (1988b) demonstrates that the same model (with identical fitting parameters) could successfully predict copper binding by a variety of fulvates isolated from different sources, indicating that source heterogeneity has a less significant effect than the conditions of the titration: pH, Cu_T, DOC, and ionic strength.

To explain ionic strength effects, consideration of the humic molecule's size and charge density are crucial. One would not expect a mixture of ligands with a charge of -1 or -2 to behave like a solution of large molecules, each having a charge of -6 or higher and containing three or more binding sites in close proximity to each other. Several models have been proposed to handle this problem: an empirical approach using some convenient functional form to describe the electrostatic effect (Tipping and Hurley, 1988), variations on Debye-Huckel and similar models (Cabaniss and Shuman,1988a), and an

empirical two-phase model which assumes a Donnan equilibrium between humic and aqueous "phases" (Ephraim and Marinsky, 1986). So far, none of these is in common use. None of them attempts to incorporate data other than the titrations themselves (such as molecular weight information or spectroscopic data). Furthermore, no model has been developed that can explain the variations in ionic strength effects over large pH ranges (three or more pH units) or ionic strength ranges (a factor of ten or more), or that explains why ionic strength effects on copper ion titrations are so much larger than effects on pH titrations.

The goal of this study is to develop an electrostatic model of humic substances that can be incorporated into simple equilibrium calculations and that can provide a chemical picture of the observed pH and ionic strength effects. There are two parts to this work. First, we compare various electrostatic models that have been proposed for polyelectrolytes and consider their applicability to humic substances. The model we choose to use must satisfy several requirements: it must be simple and based on a reasonable physical picture, require a minimum of empiricism, and draw on the wealth of available data regarding the make-up and structure of humic substances. In the second part we will attempt to model a data set showing the pH and ionic strength effects on copper binding, using a discrete ligand model combined with the electrostatic model developed in the first part. A priori information gained from spectroscopic and titrimetric data, such as the expected types and amounts of various ligands, will again make the choice of fitting parameters less arbitrary.

Our overall goal in this approach is to answer two questions: can a simple electrostatic model explain observed pH and ionic strength effects on copper-humate titrations and pH titrations? And if it can, does the model suggest new experimental approaches to improve our chances of predicting metal speciation in humate-rich natural waters?

Background -- Choice of an electrostatic model

Electrostatic models for small ions interactions with other small ions, polyelectrolytes, and charged surfaces in electrolyte solutions have been studied for many decades and give us a starting point for our model. However, none of these models directly fits our needs. Aiken and Malcolm(1987) have pointed out that the term "oligoelectrolyte" may be most appropriate for a fulvic acid molecule. With an average molecular weight of close to 1000 daltons and a strong acid content of roughly 6 meq/g, the "average" molecule will have a charge near -6, falling outside the range of both Debye-Hückel and polyelectrolyte theories.

However, a significant fraction of the molecules in a fulvate sample may have molecular weights much higher than 1000. In a flow field-flow fractionation study, believed to be more accurate for determining molecular weight distributions than more commonly used chromatographic methods, Beckett *et al.* (1987) found that typical fulvic acid samples with average molecular weights near 1000 daltons also included a large fraction (10 % or more by weight) of molecules in the 5000-10000 dalton size range. In humates approximately 5-20 % of the total mass consisted of molecules in the 10000-25000 dalton size range. These considerations lead to the conclusion that in addition to satisfying previously stated requirements of simplicity and parsimony, our model should also be able to handle a size distribution ranging from molecules almost described by Debye-Hückel theory to ones closer to true polyelectrolytes. We shall see later that the use of a size distribution of molecules instead of an average-sized molecule will greatly improve our ability to model certain ionic strength effects. With these thoughts in mind, let us examine a number of proposed models: Counterion condensation, Donnan equilibrium, and various Poisson-Boltzmann theories.

Counterion Condensation

One of the most discussed polyelectrolyte models in the biophysical chemistry literature is Manning's model of counterion condensation (Manning, 1979). The molecule is pictured as an infinitely long cylinder of infinitesimal radius, so that the only geometrical parameter is a linear charge density. The charged sites are then treated as point charges by a Debye-Hückel limiting law, and the electrostatic energy of the molecule is given by the sum of the energies of interaction of all pairs of point charges. Manning also postulates a phenomenon he calls "counterion condensation:" any counterions found in the near vicinity of the cylinder (in the condensation volume, effectively a second phase as described above) can be considered "bound" to the polyion and therefore partially neutralize its linear charge density. By considering both the entropic contributions of the free and bound counterions as well as the electrostatic contribution of the polyion to the free energy of the system, Manning derives a very simple formula predicting the extent of counterion condensation in the limit of zero ionic strength (limiting law). The most significant result of his calculations is that, under conditions where the limiting law is a good approximation, the number of bound, or condensed, counterions is independent of the bulk solution concentration. Another result is that condensation is a discontinuous phenomenon, which only occurs when the linear charge density of the polyion exceeds a certain critical value. Manning's theory seems to provide good predictions regarding a variety of polyelectrolyte properties, especially configurational and transport properties of biological macromolecules such as nucleic acids (Anderson and Record, 1982).

However, several problems make this model unsuitable for humic acid modeling. The first has already been mentioned: the picture of the molecule as an infinitely long cylinder is unrealistic for small molecules, and unable to accomodate size

distributions, which may play an important role in humic acid properties. Even if this model could be redesigned using a different geometry (unlikely, since the cylindrical symmetry is what gives it its simplicity), a second, more significant problem still remains: the model does not distinguish site-bound ions from condensed ions. Indeed in cases where a significant amount of site-binding occurs the model's thermodynamic assumptions are incorrect and its results no longer accurate (Manning 1979). Manning's model is generally viewed as a simple but limited approximation to the difficult mathematics of more complicated models it was not created to explain strong binding behavior and to use it for modeling the metal- and proton- binding properties of humic substances would be inappropriate.

Electroneutral phases (Donnan Model)

The Donnan Model is another very simple two-phase model. The name originally refers to the distribution of small ions across a semipermeable membrane when charged macromolecules are restricted to one side of the membrane. Although there is no semipermeable membrane separating the two phases in this model, the situation is similar: the polyion's charged sites are constrained to remain in the polyion "phase" (defined by the area filled by the loosely coiled, solvated polyion) while smaller ions are free to diffuse in and out from the bulk solution. Two assumptions are necessary: that the osmotic pressure terms in the expressions for chemical potential are negligible, and that both phases are electroneutral. The first assumption leads to the conclusion that

$$\left(\frac{\{X\}_i}{\{\bar{X}\}_i}\right)^{\frac{1}{Z_i}} = \lambda \qquad (1)$$

where $\{X\}_i$ and $\{\bar{X}\}_i$ are the activities of an ion X_i with charge Z_i in the bulk and polyion phases respectively, and λ is a constant for all the ions in the solution (Tanford, 1961, p.227). The second assumption allows us to solve for λ:

bulk phase electroneutrality:

$$\sum_i Z_i [X]_i = 0 \qquad (2)$$

polyion phase electroneutrality:

$$\sum_i Z_i [\bar{X}]_i + \frac{Z_p}{N V_p} = 0 \qquad (3)$$

where $[X]_i$ and $[\bar{X}]_i$ are the concentrations of X_i in the bulk and polyion phases respectively, Z_p is the charge of a polyion molecule, V_p is the phase volume occupied by the molecule, and N is Avogadro's Number. Thus, Z_p/NV_p is the density of charged sites in the polyion phase. No assumption needs to be made about the geometric shape of the polyion phase. Assuming that the activity coefficients of $[X]_i$ and $[\bar{X}]_i$ are equal and substituting equation (1) into equation (3) yields:

$$\sum_i Z_i [X]_i \lambda^{Z_i} + \rho_p = 0 \qquad (4)$$

where $\rho_p = Z_p/NV_p$, and can be calculated if ρ_p and the bulk solution concentrations of the major ions are known.

If the total concentration of monovalent ions is much greater than that of any multivalent ions (I (ionic strength) = $[Na^+]$ = $[Cl^-]$, for example), then the expression becomes much simpler:

$$\lambda = \frac{-\rho_p + \sqrt{\rho_p^2 + 4\,I^2}}{2\,I} \qquad (5)$$

Note the limiting behaviors:

λ approaches 1 if $I >> |\rho_p|$

λ approaches $-\rho_p/I$ if $|\rho_p| >> I$ and $\rho_p < 0$ (polyanion)

and λ approaches I/ρ_p if $|\rho_p| >> I$ and $\rho_p > 0$ (polycation).

Thus if $|\rho_p|$ is large compared to I, the concentration of counterions in the polyion phase is simply equal to the concentration of polyion charge, $|\rho_p|$, and is independent of ionic strength. This is reminiscient of the counterion condensation model; the difference is that in this case the condensed counterions neutralize the charge density completely in all cases (as long as $|\rho_p| >> I$) while in Manning's model they partially neutralize the charge and only condense at all if the charge density exceeds a certain value.

Another difference is that this model easily accomodates site binding. Intrinsic equilibrium constants can be written in terms of the local concentration of ions near the polyion's binding sites. Apparent equilibrium constants are then a function of λ. For example, if

$$K_{a,\,int} = \frac{\{\bar{H}^+\}\ \{\bar{A}^-\}}{\{\overline{HA}\}} \qquad (6)$$

where A^- is a weakly acidic site on the polyanion, then

$$K_{a,app} = \frac{\{H^+\}\ \{\bar{A}^-\}}{\{\overline{HA}\}} = \frac{K_{a,int}}{\lambda} \qquad (7)$$

In other words, the apparent pK_a of the polyanion is a function of λ, which is itself a function of I and pH (since ρ_p is a function of pH).

A model of this type combined with a number of proton- and or metal- binding sites has been applied to humic substances by Ephraim and Marinsky (1986). One disadvantage of this model is that there is again no easy way to account for size distributions. One could assume that ρ_p is some function of molecular weight, but this introduces another arbitrary parameter into our model, which we are trying to keep as simple and constrained by our knowledge of the problem as possible. Another disadvantage is that even if fulvic acid can be well described as a penetrable phase, the Donnan model is almost certainly inappropriate for the smaller sized molecules, as we will discuss in the following section.

Poisson-Boltzmann Theories

This category is a broad one, encompassing Debye-Hückel theory of small ions in solution, Gouy-Chapman theory for adsorption on charged surfaces, and a number of polyelectrolyte models. The Poisson-Boltzmann Equation assumes that an electrostatic potential Ψ is created by a central charge region of interest (the polyion), and that the small, mobile ions in the solution arrange themselves according to this potential. It is derived from two parts; the Poisson equation relates potential to charge density,

$$\nabla^2 \Psi = \frac{-\rho}{\varepsilon} \qquad (8)$$

(where Ψ is the electrostatic potential, ρ is the charge density, and ε the permittivity of the medium), and a Boltzmann relation for the distribution of co- and counterions in the potential field:

$$\rho_{\pm} = \sum_i Z_i \, [X]_i \, \exp\left(-\frac{Z_i \, e \, \Psi}{k \, T}\right) \qquad (9)$$

where $\rho_{\pm}$ is the charge density created by the local imbalance of co- and counterions, e is the charge of an electron, k is the Boltzmann constant, and T is the absolute temperature. Thus the distribution of mobile ions affects ρ, affecting Ψ itself. A sort of equilibrium is achieved when the distribution of charges in the potential field Ψ is consistent with the Ψ created by the mobile ions and the central charged region:

$$\nabla^2 \Psi = -\frac{(\rho_o + \rho_{\pm})}{\varepsilon} \tag{10}$$

where ρ_o is the charge in the region in the absence of mobile ions. This equation easily accomodates both one-phase and two-phase models. In a one-phase model, ρ_o is zero everywhere and the surface charge density σ of the central charged region results in the boundary condition:

$$\left(\frac{\partial \Psi}{\partial r}\right)\Big|_{r=R} = \frac{-\sigma}{\varepsilon} \tag{11}$$

where $(\partial\Psi/\partial r)|_{r=R}$ is the potential gradient at the surface (Gauss' Law). In a two phase model, ρ_o is equal to ρ_p inside the polyion phase and zero in the bulk phase. The boundary condition becomes:

$$\left(\frac{\partial \Psi}{\partial r}\right)\Big|_{r=R1} = 0 \tag{12}$$

where R1 is the center of the charged region. In both the one-phase and the two-phase models, the other boundary condition is that the potential disappears at large distances from the central charged region:

$$\lim_{r \to \infty} \Psi = 0 \tag{13}$$

Some possible problems with this approach have been discussed . The first concerns the assumption that the distribution of the mobile ions can be described by a

continuous function, ρ, representing the ions not as point charges but as "smeared" regions of charge, and that the mobile ions' only interactions with each other are coulombic and therefore included in the Poisson Equation. LeBret and Zimm (1984) have used Monte Carlo methods to demonstrate that substantial errors may arise when the local concentration of counterions is so large that non-Coulombic interactions can no longer be ignored, or when the size of the counterions is not small compared to geometrical parameters (such as the cylindrical radius) of the polyion. Another problem arises from the inadequacies of the Poisson-Boltzmann equation itself, which assumes that the potential of an average force (the Ψ of the Boltzmann relation) is the same as the average potential (the Ψ of the Poisson equation). Kirkwood (1934) shows that this is a good approximation only when $|e\Psi/kT| << 1$. However, Fixmann (1979) shows that the equation also gives reasonable results when the potentials are high, since the solution for Ψ is not very sensitive to small errors in the Boltzmann distribution. For all its shortcomings (theoretical flaws and lack of analytical solutions in all but the simplest cases), the Poisson-Boltzmann equation remains the most practical and flexible method of studying electrostatic interactions in solutions.

Analytical solutions to the Poisson-Boltzmann equation

When the potential Ψ is small, so that $\exp(e\Psi/kT) \approx 1 + e\Psi/kT$, and a one phase model is chosen, equation (10) reduces to:

$$\nabla^2 \Psi = \kappa^2 \Psi \qquad (14)$$

where κ is a constant. This linearized equation has analytical solutions for planar, cylindrical, and spherical geometries. The impenetrable sphere was first used by Debye and Hückel (1923) to derive their well-known limiting laws regarding the activity coefficients of small ions in solution.

Tanford (1961) also solved the equation for a penetrable sphere. Tanford's model has been applied to humic substances by Wershaw and Pinckney(1973). However, when Ψ is large the linear approximation is quite inappropriate -- this is a major problem with both Tanford's and Wershaw's approaches.

The only non-linear Poisson-Boltzmann equation for which an analytical solution has been found is the planar one. This solution was used by Verwey and Overbeek (1948) to model the interactions between the charged surfaces of suspended colloids, and applied by Dzombak and Morel (1990) in a surface complexation model. The latter's model resembles the Donnan formulation explained in the previous section: intrinsic equilibrium constants of various surface reactions are combined with an electrostatic factor λ to give apparent constants which are functions of surface charge density and ionic strength. Any Poisson-Boltzmann theory for which Ψ is known as a function of charge could be used in the same fashion. Since a plane is probably not a good approximation for the shape of a polyelectrolyte or a humic acid, and since analytical solutions of the non-linear form are not known for the other geometries, we have explored the idea of using a numerical solution for this purpose.

Impenetrable cylinders

A number of numerical solutions have been proposed for the infinitely long, impenetrable cylinder (for example Kotin and Nagasawa 1962 and Delville 1980), the prevalent geometry used in polyelectrolyte modeling. The resulting surface concentrations of mobile ions have also been compared to the predictions made by Manning's counterion condensation model (Bizzarri *et al.* 1988, LeBret and Zimm 1984b, Cametti and DiBiasio 1988) (see above). When comparing the two models, a somewhat arbitrary parameter has to be introduced to specify how closely the counterions have to approach the cylinder to be considered "condensed" in the Poisson-

Boltzmann formulation (which is a one-phase model). Nevertheless, the models compare quite well where Manning's assumptions are valid. However, since the Poisson-Boltzmann equation can also be applied in a much broader range of conditions, it is the more flexible of the two models, and Manning's model could be considered a simplified special case of the Poisson-Boltzmann equation (Mandel 1988).

In order to construct an impenetrable cylinder model that can handle size distributions, we could use finite cylinders of varying lengths. However, this would add another position dimension to the Poisson-Boltzmann equation, resulting in a non-linear partial differential equation that would need considerable computing power to solve numerically. We do not consider this possibility here.

Penetrable and impenetrable spheres

One might wonder why an impenetrable cylinder is almost invariably chosen to model the solvated linear polyelectrolytes most studied by biochemists. Would a penetrable sphere not be a better description of the loosely coiled molecule one might expect to see in a good solvent? This idea was considered in some early studies (Hermans and Overbeek 1948, Wall and Berkowitz 1957), but later abandoned because the potentials obtained from these models were not high enough to fit experimental data (Mandel 1988). This observation is justified by the fact that the radius of curvature of the curled, cylindrical polyion is large compared to the distance scale characteristic to the problem of polyion-small ion interactions. Other problems with larger characteristic distances do require different formulations (Mandel 1988).

Since humic substances are hardly linear polymer chains, it is not clear that the same reasoning is appropriate to their modeling. The picture of a penetrable sphere may be a better approximation. For smaller molecules an impenetrable sphere also seems likely

to be a good description. The latter would at least guarantee Debye-Hückel behavior under conditions of low potential, since it uses the same physical picture.

Furthermore, size distributions are easily handled by both models. We could assume that the molecular weight of the molecule is proportional to the cube of its radius and that all size groups have the same number of charged sites per unit weight. Then in the case of the penetrable sphere, the charge density ρ_o will not vary with size, while in the case of the impenetrable sphere the surface charge density σ will increase in direct proportion to the radius. These models require a minimum of size parameters: a molecular weight distribution (such as the ones measured by Beckett *at al.* 1987), a charge per unit weight ratio (measured titrimetrically and spectroscopically by a number of researchers) and a parameter describing the relationship between radius and molecular weight (which requires knowing the radius associated with a particular molecular weight). Data relating an average radius, measured by small angle x-ray scattering, to a (number) average molecular weight (Aiken *et al.* 1989) should give a reasonable estimate of the last parameter, since the more abundant smaller molecules should dominate both averages.

It appears that the penetrable and impenetrable sphere models both fit our requirements of simplicity and ability to handle size distributions well. Unfortunately, the non-linear forms of the equation (10) for these models do not have analytical solutions and we must resort to numerical methods in both cases. (Appendix A provides a detailed description of the methods used.)

The result of a numerical solution is Ψ as a function of r (the distance from the center of the sphere) for a given ionic strength, molecular radius R, and charge on the molecule. In the case of the impenetrable sphere, the relevant charge parameter is σ, the surface charge density on the sphere (assumed to be uniform). Figure 1 shows the results of

calculations for a variety of ionic strengths and radii. The electrostatic factor λ is analogous to that used in the Donnan model (equation 1) and is given by:

$$\lambda = \exp\left[-\frac{e\Psi_o}{kT}\right] \tag{15}$$

where Ψ_o is the value of Ψ at the surface of the sphere. Since a functional form λ versus σ is needed to carry out equilibrium calculations, we have fit the curve to a three parameter function (shown by the solid lines):

$$\sigma = a \sinh(b \log\lambda) + c (\log\lambda) \tag{16}$$

Note that the slopes of the lines at small σ (small λ) approach the slope given by the linear approximation (essentially, the Debye-Hückel solution) to the Poisson-Boltzmann equation. Also, when the radius of the molecule is much greater than the characteristic length scale of the problem ($1/\kappa$ from equation 14, or 10 Å, 32 Å, and 100 Å for ionic strengths 0.1, 0.01, and 0.001 M respectively), the curvature of the sphere becomes unimportant and the solution approaches that of the Gouy-Chapman solution for a plane (figure 2).

We now assume that the acid content of a fulvic acid is 6.1 meq/g (Bowles *et al.*, 1989), and that an average molecule has a radius of gyration of 7.7 Å and an average molecular weight of 711 daltons (Aiken *et al.*,1989). The total charge on the molecule of radius 7.7 Å is the 4.3, leading to a σ of 9.2 $\mu c/cm^2$. Assuming that the molecular weight (and hence the total charge) is proportional to the cube of the radius, we can calculate σ for other sizes, leading to figure 3, which describes the effect of size on λ. As in the case of Manning's and Donnan's models, the concentration of counterions in the vicinity of the molecule (given by λI) approaches a constant as the ionic strength decreases, so that a decrease in I of a factor of ten can never increase λ by more than a factor of ten.

It is important to note that in all of the results shown here, the variable I refers to the concentration of monovalent ions only. The traditional definition of ionic strength is only useful when the Poisson-Boltzmann equation is linear, as in the Debye-Hückel model. In a non-linear model, the presence of multivalent counterions will only be insignificant if $\lambda I >> Z_i \lambda^{Z_i} [M^{Z+}]$ (see equation (9)). For example, for a value of λ of 100 and a concentration of a monovalent salt of 0.01 M, a Ca^{2+} concentration of 10^{-4} M is sufficient to significantly affect the electrostatics of the model even though the ionic strength only changes by a few percent. In some fresh waters and especially seawater, ionic strength is likely to be a poor predictor of the effect ions such as Ca^{2+} and Mg^{2+} may have on the electrostatics of large ions in the solution.

In the case of the penetrable sphere, the relevant charge parameter is ρ_p, the charge density contained in the volume of the sphere. Figure 4 shows the model results for this geometry, analogous to figure 1 of the impenetrable sphere model. In this case,

$$\lambda = \exp\left(-\frac{e\,\Psi_{ave}}{kT}\right) \tag{17}$$

where Ψ_{ave} is an average of $\Psi(r)$ over the volume of the humic phase:

$$\Psi_{ave} = \int_{R1}^{R} \frac{3\,r^2}{R^3 - R1^3}\,\Psi(r)\,dr \tag{18}$$

This averaging of Ψ to find an average λ is strictly only correct when $\Psi(r)$ is small (so that $\exp(-e\Psi(r)/kT)$ is approximated by $1 - e\Psi(r)/kT$) or when $\Psi(r)$ is almost constant over the volume of the phase, so that $\Psi_{ave} \approx \Psi(r)$. It serves as a reasonable approximation in other cases. (This definition of Ψ_{ave} is strictly correct if λ is considered to be a work function instead of a concentration factor -- a complete description of this thermodynamic formalism is found in Appendix B.)

The solid lines in Figure 4 are a fit to the three parameter equation

$$\rho_p = a \sinh(b \log \lambda) + c (\log \lambda) \qquad (19)$$

However, instead of optimizing the fit, as we did for the impenetrable sphere, we used our knowledge of the limiting behaviors of the solution to estimate the parameters a, b, and c. When ρ_p and log λ are small, log λ is a linear function of ρ_p, its slope predicted by the Tanford model. When ρ_p and log λ become very large, the numerical solution behaves like the Donnan Model, which simply says that $\lambda = \rho_p/I$ (if $\lambda >> 1$). The function above displays the required behavior when a = 2I, b = ln(10), and 1/(c+ab) is equal to the slope $(\log \lambda)/\rho_p$ given by the Tanford model (which can be calculated directly given R and I). The solid lines in figure 4 demonstrate that this estimate is able to approximate the numerical solution to within 0.2 log units for a larger range of ionic strengths, radius, and charge density than we are likely to need.

Using the same charge density parameters that we used in the impenetrable sphere model, we find that a radius of 7.7 Å and a molecular weight of 711 daltons correspond to a charge density ρ_p of 3.7 M inside the humic phase. Since total charge and valume are both proportional to R^3, in this model the charge parameter is a constant for all size groups. Nevertheless, the effect of size on log λ is substantial in the size range of interest (5 Å - 20 Å). Figure 5 shows this effect as well as the asymptotic behavior of the function -- approaching the Tanford (linearized) model when log λ is small and the Donnan model when λ is large. Note that once the molecule is large enough to be well-described by the Donnan model (R > 30 Å or so), there is no longer a size effect on λ. Also, the effect of ionic strength on λ is once again no larger than proportional. Finally, despite the difference in the physical picture, the penetrable sphere model's results for small molecules agree closely with those predicted for the impenetrable sphere (Debye-Hückel) model.(Table 1).

Comparison of Polyelectrolyte Models

Of the different models discussed above, we have found the penetrable and impenetrable sphere models the most convenient to use in our modeling efforts. Both models can describe the effect of size distributions elegantly, and provide an "in-between" solution for molecules not described well by either Debye-Hückel or polyelectrolyte models. Their behavior converges on a Debye-Hückel type behavior for small-sized molecules (Table 1), and on either the Donnan model (penetrable spheres) or the Gouy-Chapman model (impenetrable spheres) when the radius becomes very large . In the case of penetrable spheres, the limiting behavior allows us to reliably predict the slope of the function log λ versus ρ_p without carrying out numerical solutions for each new set of conditions. For impenetrable spheres, numerical solutions must be calculated for each new radius and ionic strength, but the resulting function of log λ versus σ is well described by three parameters.

The choice between penetrable and impenetrable sphere models is at this point somewhat arbitrary. Both present a reasonable physical picture, although intuition suggests that the penetrable sphere is more appropriate for larger molecules while the impenetrable sphere (with a surface charge density proportional to its radius) is probably only a reasonable approximation of smaller molecules. Comparison of figures 3 and 5 shows that in the size range of interest (5 Å to 20 Å), and especially in the lower part of this range, the predicted log λ does not greatly differ from one model to the other. Although the penetrable sphere model is more convenient computationally, we have chosen to use the impenetrable sphere in the modeling to follow. Both the values of log λ and the size effect in the 5 Å to 20 Å size range are larger for this model, which will prove to be an advantage in the modeling of ionic strength effects on copper and hydrogen ion titrations.

The ability of these models to predict observed behavior of humic substances will be discussed in the next section.

It is important to realize, however, that the seemingly very different types of electrostatic models discussed in this section are all indistinguishable from each other in some sense. All of the models exhibit the behavior first discussed in relation to Manning's model: that λ is proportional to 1/I at sufficiently low ionic strengths and sufficiently high charge densities, so that the local concentration of counterions eventually reaches some value that no longer varies with ionic strength. The predicted absolute values of λ, and the amount of neutralization of polyion charge by counterions, vary from model to model, but if we have no a priori information concerning the magnitude of intrinsic binding constants, the observation that λ is proportional to 1/I or that $K_{a,app}$ is proportional to I for some reaction does not alone suffice to let us distinguish between penetrable and impenetrable, or spherical and cylindrical geometries, or differing thermodynamic pictures.

Modeling Work

Now that we have chosen a model and explored its basic characteristics, we can study the data sets and ask ourselves whether or not our chosen model is able to explain the observed effects. We wish our model to exhibit the pH and ionic strength effects on titrations of Suwannee River Fulvic Acid with Cu^{2+}(figure 6) measured by S. E.. Cabaniss (1986), while at the same time showing the lack of ionic strength effect observed in pH titrations (pers. comm., D.M.McKnight and S.E. Cabaniss).

Our computational techniques have been adapted from the Diffuse Layer Model version of J. C. Westall's BASIC computer program MICROQL (1979). In addition to copper-fulvate complexes, the inorganic species $Cu(OH)^+$ and $Cu(OH)_2$ were included in the equilibrium calculations, using the formation constants compiled in Morel (1983). Inorganic complexes of copper with the buffer ions (1 mM PO_4 in the pH 7.00 titrations and 1 mM CO_3 in the pH 8.44 titrations) were found to be insignificant. Precipitation of solids was not considered although it should be noted that at high pH, the solution was oversaturated with $Cu(OH)_{2\,(s)}$ at copper concentrations up to a factor of ten lower than those at which Cabaniss (1986) could detect the presence of precipitates and stopped the titration. In the modeling that follows, pCu and pCu_T refer to $-\log[Cu^{2+}]$ and $-\log[Cu_T]$ (concentration scales), while pH refers to $-\log\{H^+\}$ (activity scale). Solution activity coefficients were estimated using the Davies equation with A = -1.17 and b = 0.24 (Morel, 1983).

Our forward modeling approach consists of beginning with an oversimplified model (one size group, one copper binding site) and exploring how closely we can fit the data by varying the model's parameters. We then consider how the model fails and why, and add complexity stepwise, reasoning at each step how the next level of complexity should

improve the fit. Our goal is not to an optimized fit of the data set but a concise explanation of the observed pH and ionic strength effects.

The features of figure 6 to be explained are:

- the general "smeared" appearance of the curves (slope of pCu vs. $pCu_T \approx 2$ over 1.5 orders of magnitude).

- the lack of binding and the small ionic strength effect at pH 5.14.

- the very large ionic strength effect (almost 2 orders of magnitude for a tenfold change in ionic strength) at pH 7.

- a smaller ionic strength effect (approximately one order of magnitude) at pH 8.44.

- the large pH effect at ionic strength 0.1 M (at low Cu_T, 1.6 log units as pH varies from 5.14 to 7.00, and also 1.6 log units as pH varies from 7.00 to 8.44).

- varying pH effects at ionic strength 0.01 M (at low Cu_T, 3.0 log units as pH varies from 5.14 to 7.00 and only 0.9 log units as pH varies from 7.00 to 8.44).

To understand how λ relates to pH and ionic strength effects, we must consider how an apparent copper binding constant may be formulated under different conditions. For a diprotic site, three cases are possible: binding copper to the site may release two protons, one proton, or no proton, depending on the acidity constants of the site and the pH of the solution. It is convenient to define an intrinsic binding constant of the humate site to a divalent solution ion (M^{2+}) in terms of the humate site concentrations and a

"local" ion activity $\{M^{2+}\} = \lambda^2 \{M^{2+}\}$. The intrinsic copper binding constant of site A" is then defined as:

$$K_{Cu,\,int} = \frac{[CuA]}{[A^{2-}]\ \{\bar{C}u^{2+}\}} \qquad (20)$$

Similarly, intrinsic pK_a's are

$$K_{a1,\,int} = \frac{\{\bar{H}^{+}\}\ [A^{2-}]}{[HA^{-}]} \qquad K_{a2,\,int} = \frac{\{\bar{H}^{+}\}\ [HA^{-}]}{[H_2A]} \qquad (21)$$

We define the "apparent" copper binding constant for this site as

$$K_{Cu,\,app} = \frac{[CuA]}{[A_T - CuA]\ \{Cu^{2+}\}} \qquad (22)$$

Assuming that $Cu_T << A_T$, the quantity $[A_T - CuA]$ is approximately equal to $[A_T]$. Depending on the pK_a's of the site and the pH (or "local" pH, given by pH - log λ),

(a) $A_T \approx [H_2A]$ if $p\bar{H} < pK_{a2,\,int}$

(b) $A_T \approx [HA^{-}]$ if $pK_{a1,\,int} > p\bar{H} > pK_{a2,\,int}$

(c) $A_T \approx [A^{2-}]$ if $p\bar{H} > pK_{a1,\,int}$ (23)

This leads to three possible expressions for $K_{Cu,app}$:

(a) $K_{Cu,\,app} = \dfrac{K_{Cu,\,int}\ K_{a1,\,int}\ K_{a2,\,int}}{\{H^{+}\}^2}$ if $p\bar{H} < pK_{a2,\,int}$

(b) $K_{Cu,\,app} = \dfrac{K_{Cu,\,int}\ K_{a1,\,int}\ \lambda}{\{H^{+}\}}$ if $pK_{a1,\,int} > p\bar{H} > pK_{a2,\,int}$

(c) $K_{Cu,\,app} = K_{Cu,\,int}\ \lambda^2$ if $p\bar{H} > pK_{a1,\,int}$ (24)

In other words, when the site is more deprotonated, competition with H^+ becomes less of a factor since fewer protons are exchanged in the reaction, but the electrostatic factor λ

becomes more significant since more charge is exchanged. Thus it would be reasonable to expect the ionic strength effect to increase and the pH effect to decrease with increasing pH.

This expected effect occurs in the modeling attempt shown in Figure 7. To construct this model, we assumed that carboxylic acids are the prevalent acidic sites and that two carboxylic acids in close proximity to each other (such as a phthalic acid) are the prevalent copper binding sites. K_a's and K_{Cu}'s were chosen to reflect this assumption (Table 2); total ligand concentrations are consistent with the titrimetric measurements of Bowles *et al.*(1989) and the spectrometric measurements of Noyes and Leenheer (1989), who measured total carboxyl contents of Suwannee River Fulvic Acid at 6.1 meq/g and 6.8 meq/g respectively. To keep the model simple, the monoprotic acid site was assumed to create charge density only and not to affect the copper binding (although at the high copper loadings characteristic of some data sets, a weak site such as acetate or benzoate could play a significant role).

Figure 7 demonstrates that this one-site model has other flaws besides its expected inability to produce the pH and ionic strength effects observed in the data. The titrations are not "smeared", reflecting the fact that only one binding site dominates the binding. To see reasonably large ionic strength effects, a molecular weight much larger than the measured averages had to be used. Finally, a pH titration of the same model (figure 8) shows large ionic strength effects. Like the pH and ionic strength effects on copper titrations, this was also to be expected. The largest effect electrostatics can have on $K_{Cu,app}$ is a factor of λ^2, while the smallest effect we would see on the $K_{a,app}$ is a factor of λ. To model the ionic strength effect at pH 7, we need λ to increase by about a factor of ten as the ionic strength is decreased from 0.1 to 0.01 M — and this factor of ten produces significant effects indeed on the pH titration (which is on a linear scale). Note

also that according to our conclusions of the previous section, the factor of ten is the largest possible ionic strength effect on λ.

In the context of Poisson-Boltzmann models, there is only one way that the electrostatics could have such a large effect on Cu titrations and such a small one on pH titrations: the fulvic acid must be a mixture of substances with different electrostatic properties, one of which dominates the H^+ binding and the other the Cu^{2+} binding. This situation is most simply and logically produced by using a size distribution of molecules. As shown below, even if the content of acidic and copper binding sites remains constant from one molecular size to another, a small amount of large molecules with large values of λ can dominate the Cu^{2+} binding while a larger amount of smaller molecules with a small λ will dominate pH titrations.

Figures 9 and 10 were produced using a mixture of two size groups. The ratio of molecular weights used produces a polydispersity of 2.0, within the range of Beckett *et al.*'s measurements. Note also that the number average molecular weight is now 907, in closer agreement with the measurements, and that the Cu^{2+} titrations appear more smeared than in figure 2, because the same copper binding site distributed among two size groups behaves like two sites of different strengths and concentrations.

However, introducing two size groups has not solved the problem of pH and ionic strength effects. We can greatly improve our model fit by simply introducing another binding site. Examination of figure 9 suggests that the titration most out of place is the one at pH 8.44 and ionic strength 0.1 M. Introducing a binding site which becomes significant only under these conditions may solve the problem. A diprotic site such as catechol does not significantly deprotonate in the pH range of interest. Its apparent binding constant is hence governed by equation 24a. When incorporating this new type of site into our model, we are again guided by the titrimetric data of Bowles *et al.*(1989)

and the spectrometric data of Noyes and Leenheer(1989), reporting phenolic OH contents in Suwannee River Fulvic Acids of 1.2 meq/g and 1.4 meq/g ("reactive" phenolic OH) respectively. Our chosen value of 0.53 mM/g catechol content is not incompatible with these figures, although it suggests that almost all of the phenolic sites are paired in a catechol-type site.

When a site of this kind is added to the model, its behavior is much closer to that exhibited by the data (figure 11), while the pH titration (figure 12) remains unaffected. Note, however, that the copper titrations at high pH become sharp again instead of smeared. Since the diprotic site dominating at this pH is not affected by electrostatics (see equation 24a), the two size groups do not appear as two sites of apparently different strengths. A third binding site, which again only becomes significant at high pH's, may be needed to produce the smearing.

Although we could add more binding sites or size groups to smoothe out figure 11 a bit, the two-site, two-size group model does meet our initial requirement of explaining the major pH and ionic strength effects concisely. It is now possible to consider what advantages the impenetrable sphere model provides over the penetrable sphere. First, the "smeared" look of the titration curve results when most of the copper is bound by the largest size group at low copper loading, and the smaller size group becomes significant only when the binding sites on the larger molecules have been titrated. Since the size effect on log λ is smaller in the penetrable sphere model, the difference in apparent binding strength of the sites in the two size groups is smaller, and the larger size no longer dominates the binding at low copper loading. One could partially compensate for this by increasing the ratio of large to small molecules, but this would stretch the limit placed on polydispersity by Beckett *et al.*'s measurements (1987) and also decrease the difference in ionic strength effect between Cu and pH titrations.

The second advantage of the impenetrable sphere model is that the larger log λ values lead to slightly smaller values of intrinsic K_{Cu}'s. Table 2 shows that the K_{Cu}'s required to model the observed magnitude in copper binding are already larger than would be expected from the literature values of phthalic acid and catechol; using the penetrable sphere model would have increased this discrepancy further.

However, comparing intrinsic constants in electrostatic models to literature constants is not as straightforward as it may seem: one problem is that the "ideal" thermodynamic state (activity coefficient = 1) in this electrostatic model is one where Ψ approaches zero, or at infinite ionic strengths. Literature constants follow the convention of defining an ideal state of ionic strength zero (see Appendix B). Since the non-linear Poisson-Boltzmann equations we used predict that $|\Psi|$ approaches infinity as the ionic strength approaches zero (so that the local concentration of counterions does not vary with ionic strength) and since interactions other than electrostatic ones become significant at high ionic strengths, it is not clear how the intrinsic and literature constants should be compared. Furthermore, literature constants are given in terms of molecular reactions whereas the model's constants refer to specific site's reactions (see Tanford 1961 for a discussion of this difference). Given these problems, the agreement between literature constants for expected binding sites, and the intrinsic constants of the model is not bad, although the correlation is certainly not strong enough to provide evidence for specific types of functional groups or to distinguish one electrostatic model from the other.

Conclusion

We have shown that a very simple oligo-electrolyte model with two size groups, two copper binding sites, and one additional acidic site can do very well in modeling the non-intuitive pH and ionic strength effects seen in the data. For example, it is not necessary to invoke irreversible effects such as size changes ("unfolding") or esterification to explain the smaller than expected ionic strength effects on copper binding at high pH's. Our model also suggests that it is sufficient to assume that only oxygen-containing binding sites, with their binding strengths enhanced by an electrostatic effect, are significant copper complexants in the range of copper-humate ratios studied here. Finally, we have shown that at least two size groups of molecules are necessary to explain the difference in ionic strength effects observed in pH and Cu^{2+} titrations. Our forward modeling approach successfully incorporated a variety of available data concerning the molecular weight distribution, size, and functional group content of humic substances, resulting in a parsimonious, chemically plausible description of the humate molecule.

To measure the conciseness of the model, we can count the number of fitting parameters used: 7 equilibrium constants (2 K_{Cu}'s and 5 K_a's), 3 total ligand concentrations, and 4 size parameters (the two radii, the concentration ratio of large to small molecules, and one parameter describing the size to charge density relationship), for a total of 14. However, the two K_a's of the catechol-type site are arbitrary, since the same results would be achieved as long as the pK_a's are both greather than 8.5. We used the value of 6.1 meq/g measured by Bowles *el al.*(1989) as the total content of carboxylic acid sites, reducing the number of ligand concentration parameters to two. The smaller radius (7.7 Å) was measured by Aiken *et al.* (1989) and the size to charge density relationship was calculated using given molecular weight and acid content data. These considerations

reduce the number of fitting parameters to nine. Furthermore, the other size parameters and the total concentration of catechol-type sites are not arbitrary, since they are also limited by measurable quantities (polydispersity and total phenol content). We have done quite well modeling copper titration data and, the ionic strength effect on pH titrations, using fewer fitting parameters than Cabaniss and Shuman's 5 binding site model (1988a). This model used a total of 15 parameters: 5 unconstrained K_{Cu}'s and total ligand concentrations,and five "protonicities", although one could argue that the last of these, which could only take on values of 0, 1, or 2, should not be counted fully.

The ultimate test of a model is its ability to predict as well as to explain. Surprisingly little data showing large ionic strength effects on metal-humate binding have been published; we predict that further experiments under the right conditions will confirm Cabaniss' results (1986). The belief that ionic strength effects are in general not large still prevails, despite the evidence to the contrary. One reason for this is that at the conditions of high metal loading studied in most cases, one would not expect to see large ionic strength effects: both the binding sites on the larger molecules and the diprotic sites will already be titrated. When the more abundant monoprotic weak binding sites (such as acetate) on the smaller molecules are dominating the binding, the ionic strength effect must be similar to that observed in the pH titrations, and could easily be described by Debye-Hückel activity coefficients. Since the "right" conditions for seeing large ionic strength effects are also the conditions most likely found in natural waters, more studies need to be carried out at low metal loading.

Based on our educated guesses about the types of functional groups dominating the binding under various conditions, we can also make predictions regarding metals other than Cu^{2+}. Cd^{2+}, for example, is not strongly bound by catechol-type sites. If our two-site model is sufficient for describing Cd^{2+} complexation with humates, we should see increasing ionic strength effects and decreasing pH effects with increasing pH in Cd^{2+}

titrations. In solutions containing both Cd^{2+} and Cu^{2+} ions, we would expect strong competition at low ionic strengths and pH's, when the phthalate site dominates the binding of both metals. At high ionic strengths or pH's, when the catechol site will dominate the Cu^{2+} binding while the phthalate site dominates the Cd^{2+} binding, there should be less competition. Contrary to these expectations, Fish (1984) saw only relatively weak competition of Cd^{2+} for copper binding sites at pH 6 and ionic strength 0.001 M. However, it is difficult to interpret possible electrostatic effects in an experiment that was only conducted at one pH and one ionic strength. A data set comparing metal binding competition in a range of ionic strength and pH conditions would provide some valuable insights into the issues discussed above. Since the presence of competing metals is the norm in natural waters rather than the exception, experiments such as these will provide crucial information for the development of predictive models.

Doubts remain that predictive models of metal-humate interactions based on laboratory data will ever be applicable to natural waters. Under each new set of conditions, ligand types may become significant which were invisible in other experiments. However, we are encouraged by our attempts to build a simple model capable of explaining a variety of phenomena, and we are looking forward to seeing new data sets to test and challenge our predictions.

Bibliography

Aiken, G. R.; Brown P. A.; Noyes, T. I.; Pinckney, D. J. In *Humic Substances in the Suwannee River, Georgia: Interactions, Properties, and Proposed Structures*; Averett, R. C.; Leenheer, J. A.; McKnight, D. M.; Thorn, K. A., Eds.; U. S. Geological Survey Open File Report 87-557, 1989, pp 163-178.

Aiken, G. R.; Malcolm, R. L. *Geochim. Cosmochim. Acta* **1987**, 51, 2177-2184.

Anderson C. F.; Record, M. T. *Ann. Rev. Phys. Chem.* **1982**, 33, 191-222.

Beckett, R.; Zue, Z.; Giddings, J. C. *Environ. Sci. Technol.* **1987**, 21, 289-295.

Bizzarri, A. R.; Cametti, C.; DiBiasio, A. *Ber. Bunsenges. Phys. Chem.* **1988**, 92, 17-21.

Bowles, E. C.; Antweiler, R. C.; MacCarthey, P. In *Humic Substances in the Suwannee River, Georgia: Interactions, Properties, and Proposed Structures*; Averett, R. C.; Leenheer, J. A.; McKnight, D. M.; Thorn, K. A., Eds.; U. S. Geological Survey Open File Report 87-557, 1989, pp 205-229.

Buffle, J.; Greter, F. L.; Haerdi, W. *Anal. Chem.* **1977**, 49, 216-222.

Cabaniss, S. E. Ph. D. Thesis, Harvard University, Cambridge, MA, 1986.

Cabaniss, S. E.; Shuman, M. S. *Geochim. Cosmochim. Acta* **1988**, 52, 185-193.

Cabaniss, S. E.; Shuman, M. S. *Geochim. Cosmochim. Acta* **1988**, 52, 195-200

Cametti, C.; DiBiasio, A. *Ber. Bunsenges. Phys. Chem.* **1988**, 92, 1089-1094.

Debye; Hückel. *Phys. Zeits.* **1923**, 24, 185.

Delville, A. *Chem. Phys. Let.* **1980**, 69, 386-388.

Dzombak, D. A.; Morel, F. M. M. *Surface Complexation Modeling: Hydrous Ferric Oxide*; Wiley: New York, 1990.

Ephraim, J.; Marinsky, J. A. *Environ. Sci. Technol.* **1986**, 20, 367-376.

Fish, W. Ph. D. Thesis, Massachusetts Institute of Technology, Cambridge, MA, 1984.

Fixmann, M. *J. Chem. Phys.* **1979**, 70, 4995-5005.

Hermans, J. J.; Overbeek, J. Th. G. *Rec. Trav. Chim. Pays-Bas* **1948**, 67, 761-776.

Kirkwood, J. G. *J. Chem. Phys.* **1934**, 2, 767-781.

Kotin L.; Nagasawa, M. *J. Chem. Phys.* **1962**, 36, 873-879.

LeBret, M.; Zimm, B. H. *Biopolymers* **1984**, 23, 271-285.

LeBret, M.; Zimm, B. H. *Biopolymers* **1984**, 23, 287-312.

Mandel, M. In *Encyclopedia of Polymer Science and Engineering*, Vol.11; Mark, H. F.; Bikales, N. M.; Overberger, C. G.; Menges, G., Eds.; Wiley: New York, 1988; pp 739-829.

Manning, G. S. *Acc. Chem. Res.* **1979**, 12, 443-449.

Mantoura, R. F. C.; Riley, J. P. *Anal. Chim. Acta* **1975**, 78, 193-200.

Martell, A.E.; Smith, R. M. *Critical Stability Constants*, volume 3; Plenum: New York, 1977.

Morel, F. M. M. *Principles of Aquatic Chemistry*; Wiley: New York, 1983.

Noyes, T. I.; Leenheer, J. A. In *Humic Substances in the Suwannee River, Georgia: Interactions, Properties, and Proposed Structures*; Averett, R. C.; Leenheer, J. A.; McKnight, D. M.; Thorn, K. A., Eds.; U. S. Geological Survey Open File Report 87-557, 1989, pp 231-250.

Perdue, E. M.; Lytle, C. R. In *Aquatic and Terrestrial Humic Materials*; Christman, R. F.; Gjessing, E. T., Eds.; Ann Arbor Science: Ann Arbor, MI, 1983; pp 295-313.

Press, W. H.; Flannery, B. P.; Taukolsky, S. A.; Vetterling, W. T. *Numerical Recipes*; Cambridge University Press: Cambridge, 1986.

Sunda, W. G.; Hanson, P. J. In *Chemical Modeling of Aqueous Systems*; Jenne, E. A., Ed.; American Chemical Society: Washington, DC, 1979; ACS Symp. Ser. No. 93, pp 147-180.

Tanford, C. *Physical Chemistry of Macromolecules*; Wiley: New York, 1961.

Tipping, E.; Hurley, M. A. *J. Soil Sci.* **1988**, 39, 505-519.

Verwey, E. J. W.; Overbeek, J. Th. G. *Theory of the Stability of Lyophobic Colloids*; Elsevier: Amsterdam, 1948.

Wall, F. T.; Berkowitz, J. *J. Chem. Phys.* **1957**, 26, 114-122.

Wershaw R. L.; Pinckney D. J. *J. Res. U. S. G. S.* **1973**, 1, 701-707.

Westall, J. C. "MICROQL II. Computation of Adsorption Equilibria in BASIC," Technical Report, Swiss Federal Institute of Technology, EAWAG: Dübendorf, Switzerland, 1979.

Wilson, D. E.; Kinney, P. *Limnol. Oceanogr.* **1977**, 22, 281-289.

Table 1. Comparison of electrostatic factors log λ derived from:

(a) a linearized Poisson-Boltzmann equation of an impenetrable sphere (essentially the Debye-Hückel model, but without correction for the electrostatic potential at the limit of zero ionic strength -- see Appendix B)

(b) non-linear Poisson-Boltzmann equation of an impenetrable sphere (numerical solution)

(c) non-linear Poisson-Boltzmann equation of a penetrable sphere (numerical solution)

		I 0.1 M	I 0.01 M	I 0.001 M
R = 3 Å	(a)	0.79	0.94	1.0
Z = 1	(b)	0.77	0.93	0.99
	(c)	0.89	1.1	1.1
R = 9 Å	(a)	0.18	0.27	0.32
Z = 1	(b)	0.18	0.26	0.31
	(c)	0.20	0.32	0.35

Table 2. Total ligand concentrations (per 5 mg/l C), intrinsic equilibrium constants, and, for comparison, literature constants, of the binding sites used in the modeling work. Where two size classes are present, the total amount of ligand in each size class is determined by the weight fraction of that size class. Literature constants were taken from Morel (1983). Catechol constants are from Martell and Smith (1977), corrected for ionic strength as in Morel (1983).

Model	pH$_a$	log L_T	pK_{a1}	pK_{a2}	pK_{Cu}	log L_T	pK_{a1}	pK_{a2}	pK_{Cu}	log L_T
Fig. 7/8	3.8	-4.40	4.5	4.5	4.5	-5.00	- -	- -	- -	- -
Fig.9/10	3.8	-4.40	4.5	4.5	5.1	-5.00	- -	- -	- -	- -
Fig.11/12	3.8	-4.40	4.5	4.5	5.1	-5.00	9.40	12.60	14.68	-5.28
literature constants	4.76 (acetate)		2.55	5.41	4.0 (phthalate)		9.40	13.44	14.78 (catechol)	

Figure 1. The electrostatic factor log λ of impenetrable spheres as a function of negative surface charge density σ for various radii (R in Å). Triangles, squares and diamonds represent numerical solutions for ionic strengths 0.001 M, 0.01 M, and 0.1 M respectively. Lines represent fits to equation (16). The parameters a, b, and c in each case are:

R (Å)	Ionic strength (M)	a	b	c
7.7	0.001	0.01866	1.737	5.782
	0.01	0.1966	1.549	6.403
	0.1	1.201	1.457	7.890
10.0	0.001	0.03138	1.616	4.596
	0.01	0.2523	1.499	5.098
	0.1	1.410	1.416	6.413
15.0	0.001	0.04762	1.568	3.104
	0.01	0.3214	1.474	3.625
	0.1	1.426	1.459	4.965
20.0	0.001	0.07375	1.480	2.375
	0.01	0.4862	1.352	2.749
	0.1	2.173	1.298	3.511
50.0	0.001	0.1626	1.327	1.029
	0.01	0.7735	1.248	1.209
	0.1	2.873	1.224	1.577
100	0.001	0.2213	1.267	0.5495
	0.01	0.9359	1.205	0.6360
	0.1	3.184	1.197	0.8730

Figure 1

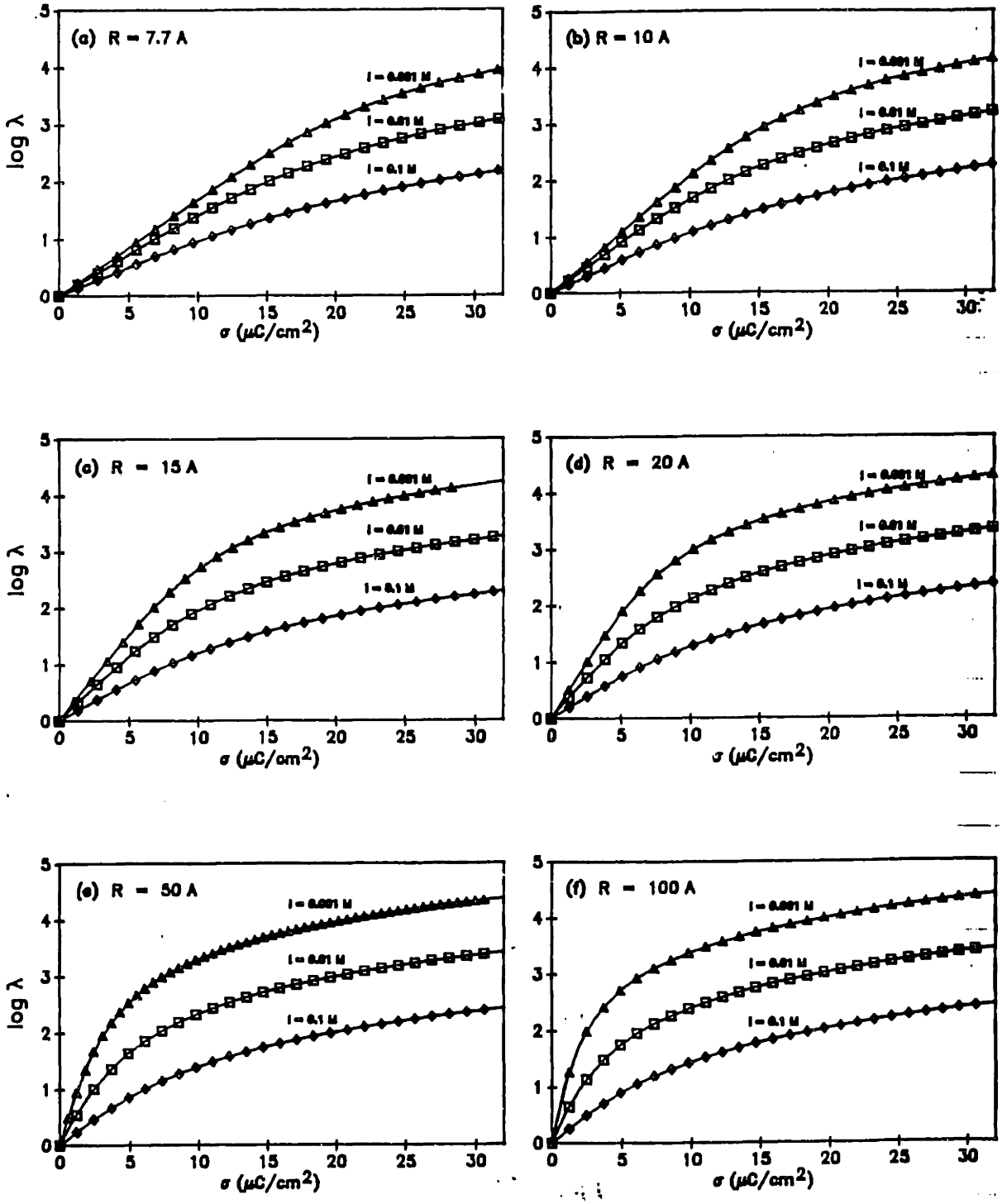

Figure 2. The analytical solution of the Poisson-Boltzmann equation of a plane (Gouy-Chapman model), log λ as a function of negative surface charge density σ. λ is again defined as $\exp(-e\Psi_0/kT)$, where Ψ_0 is the potential at the surface of the plane.

Figure 2

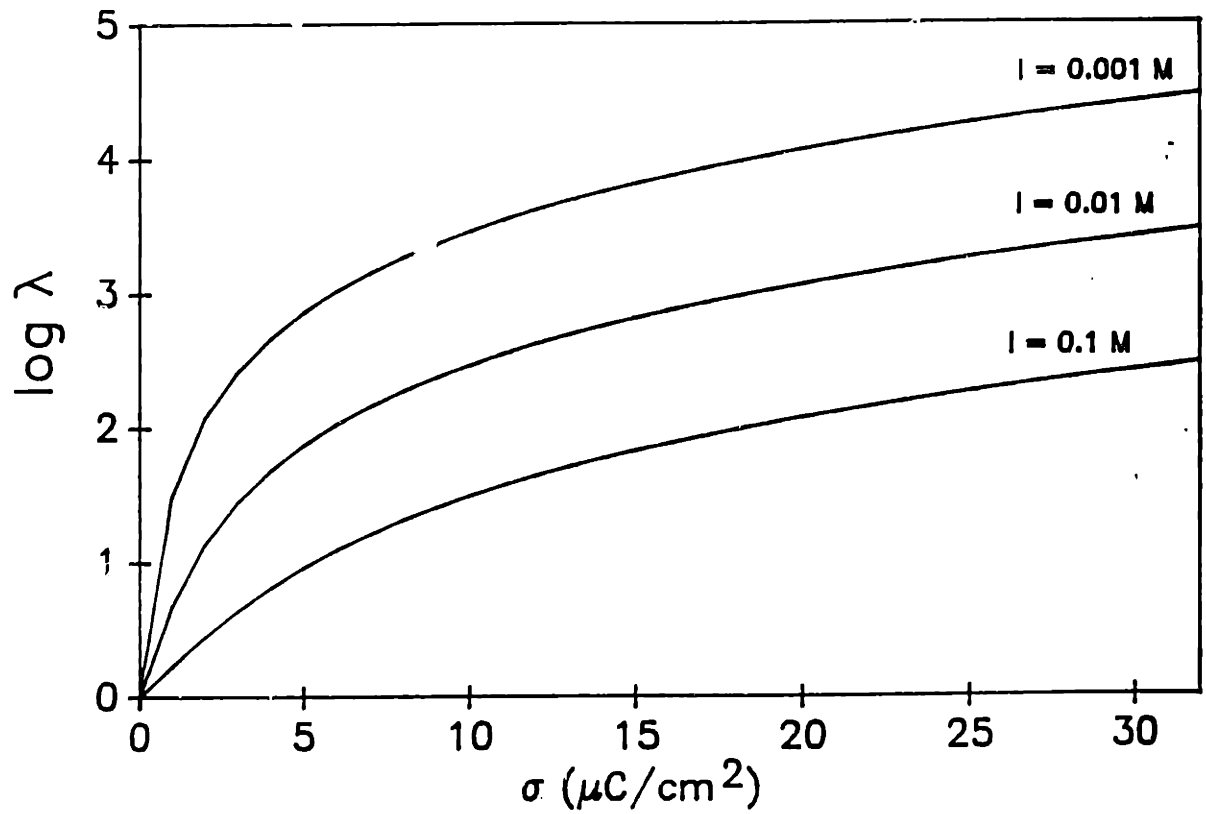

Figure 3. The electrostatic factor log λ of an impenetrable sphere as a function of radius and ionic strength. It is assumed that total charge is proportional to R^3, so that the charge density σ is increasing proportionally to R. A charge density of 9.2 $\mu C/cm^2$ was chosen for a radius of 7.7 Å, consistent with the measurements of fulvic acid molecular weight, size, and charge by Aiken *et al.*(1989.) and Bowles *et al.*(1989).

Figure 3

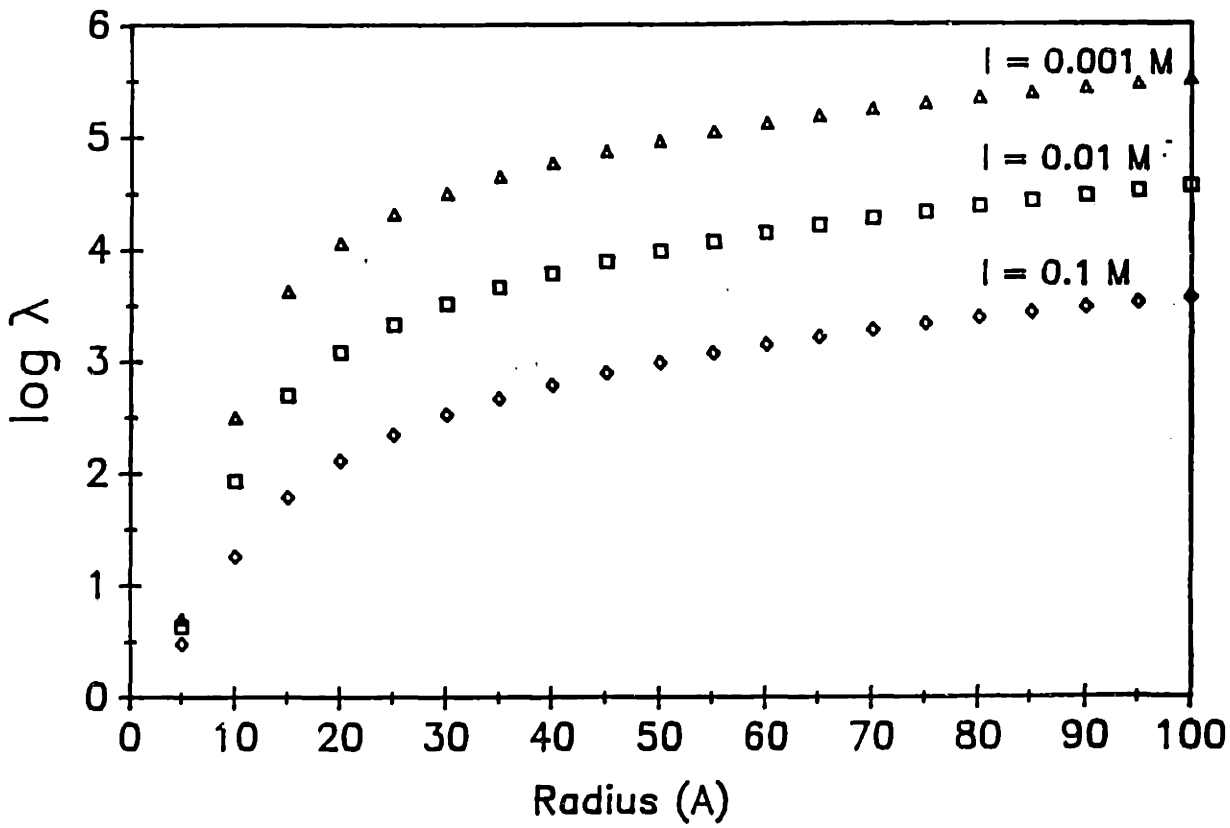
log λ
Radius (A)
I = 0.001 M
I = 0.01 M
I = 0.1 M
0
1
2
3
4
5
6
0
10
20
30
40
50
60
70
80
90
100

Figure 4. Numerical solutions of the Poisson-Boltzmann equation for a penetrable sphere. In this case, λ is given by $\exp(-e\Psi_{ave}/kT)$, where Ψ_{ave} is a potential average over the volume of the sphere. Charge density ρ_p inside the spherical volume is given in terms of moles/l. Solid lines are functions of the form $\rho_p = a \sinh(b \log \lambda) + c(\log \lambda)$, with $a = 2I$ (where I is ionic strength in moles/l), $b = \ln(10)$, and $1/(c+ab)$ is equal to the slope $(\log \lambda)/\rho_p$ calculated from the analytical solution of the linearized form of the Poisson-Boltzmann equation (Tanford, 1961).

Figure 4

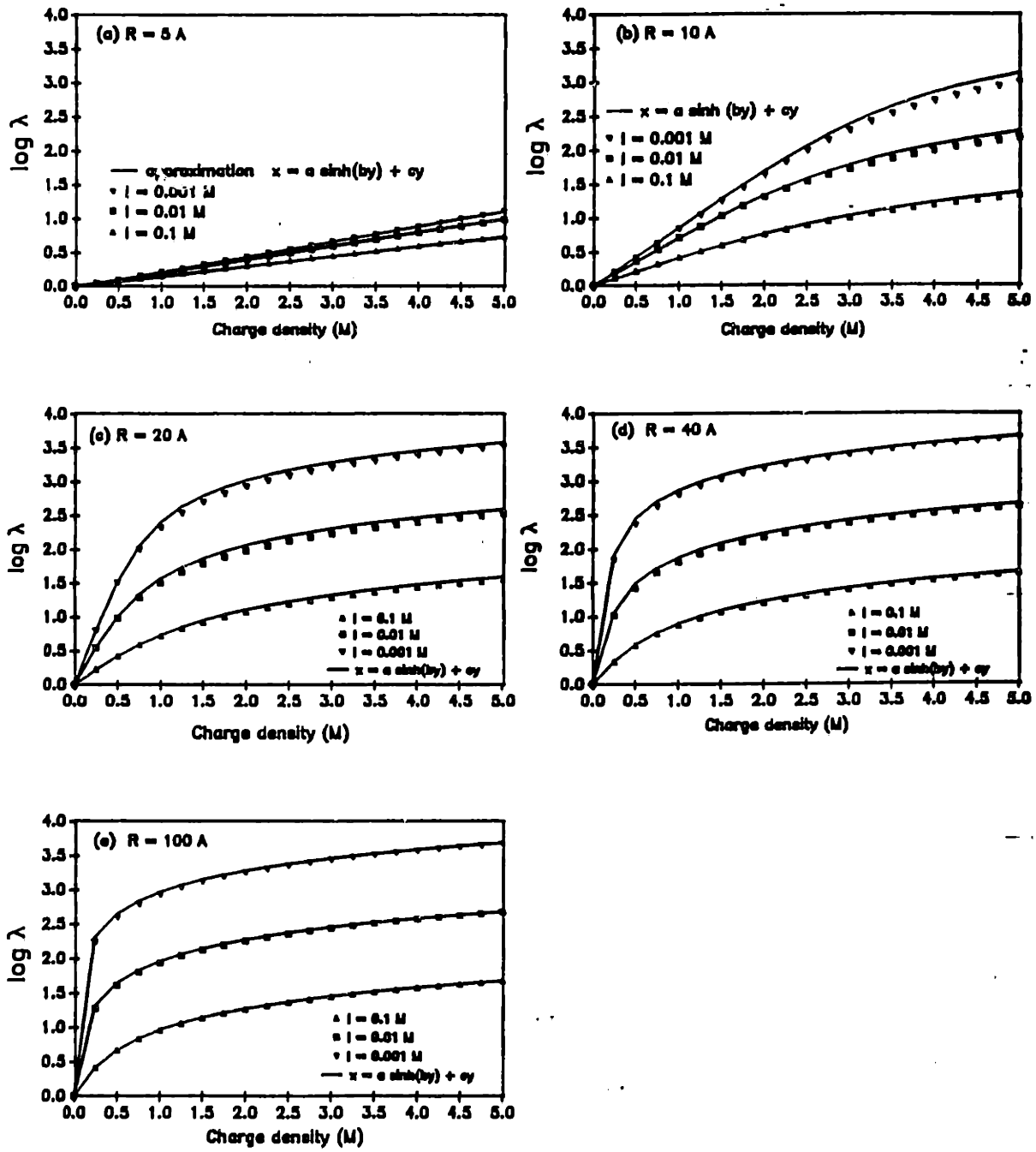
(a) R = 5 A
(b) R = 10 A
(c) R = 20 A
(d) R = 40 A
(e) R = 100 A
log λ
Charge density (M)
— approximation x = a sinh(by) + cy
— x = a sinh (by) + cy
▾ I = 0.001 M
■ I = 0.01 M
▲ I = 0.1 M

Figure 5. The electrostatic factor log λ of a penetrable sphere as a function of radius R and ionic strength I. Dashed lines represent the "Donnan" limit (electroneutrality in the charged phase). Since total charge is assumed proportional to R^3, the charge density ρ_p is not a function of radius. A value of 3.7 M was chosen, again consistent with measurements of fulvic acid molecular weight, size and charge by Aiken *et al.*(1989) and Bowles *et al.*(1989).

Figure 5

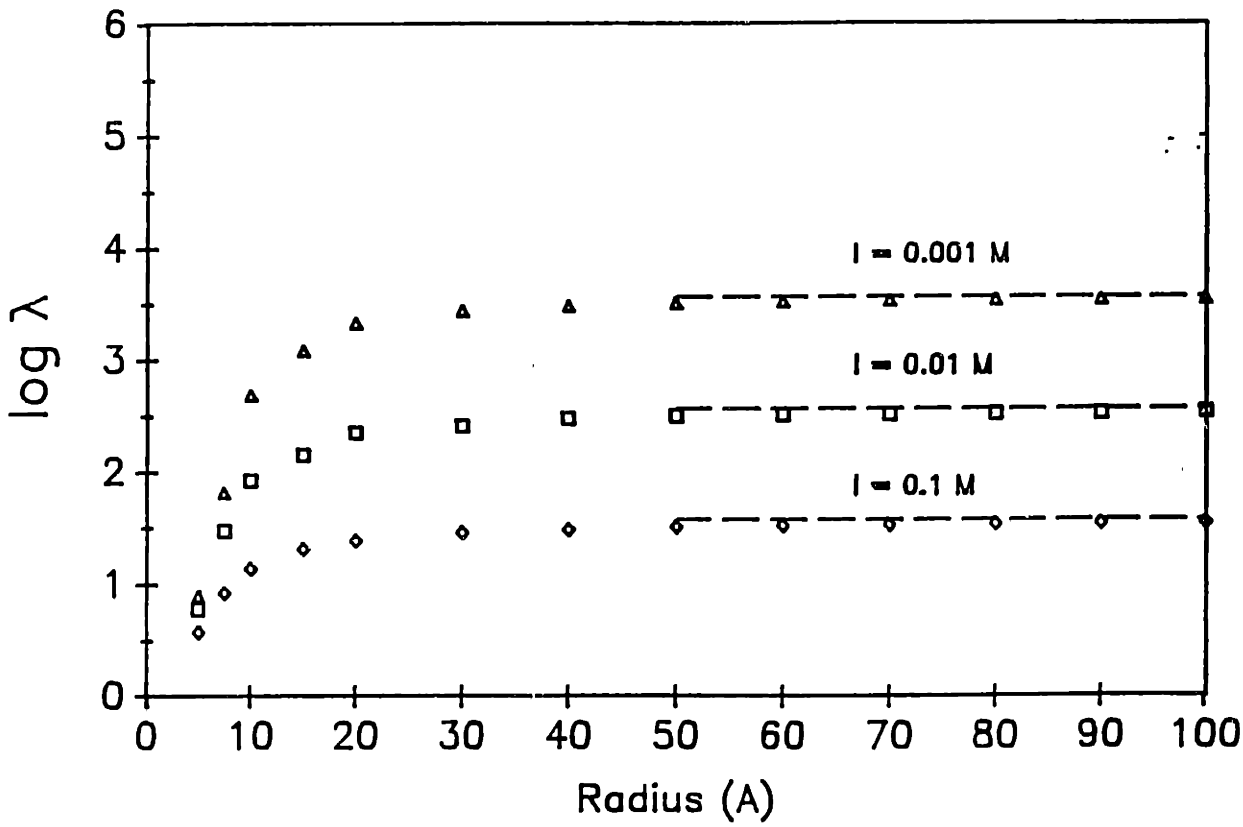
log λ
6
5
4
3
2
1
0
I = 0.001 M
I = 0.01 M
I = 0.1 M
0
10
20
30
40
50
60
70
80
90
100
Radius (A)

Figure 6. The Cu^{2+} titration data collected by S. E. Cabaniss (1986). The plot shows pCu versus pCu_T (concentration scales) at three different pH's (5.14 -- squares, 7.00--triangles, and 8.44--inverted triangles) and two ionic strengths: I 0.01 M (filled symbols) and I 0.1 M (open symbols), in the presence of 5 mg C/l Suwannee River Fulvic Acid.

Figure 6

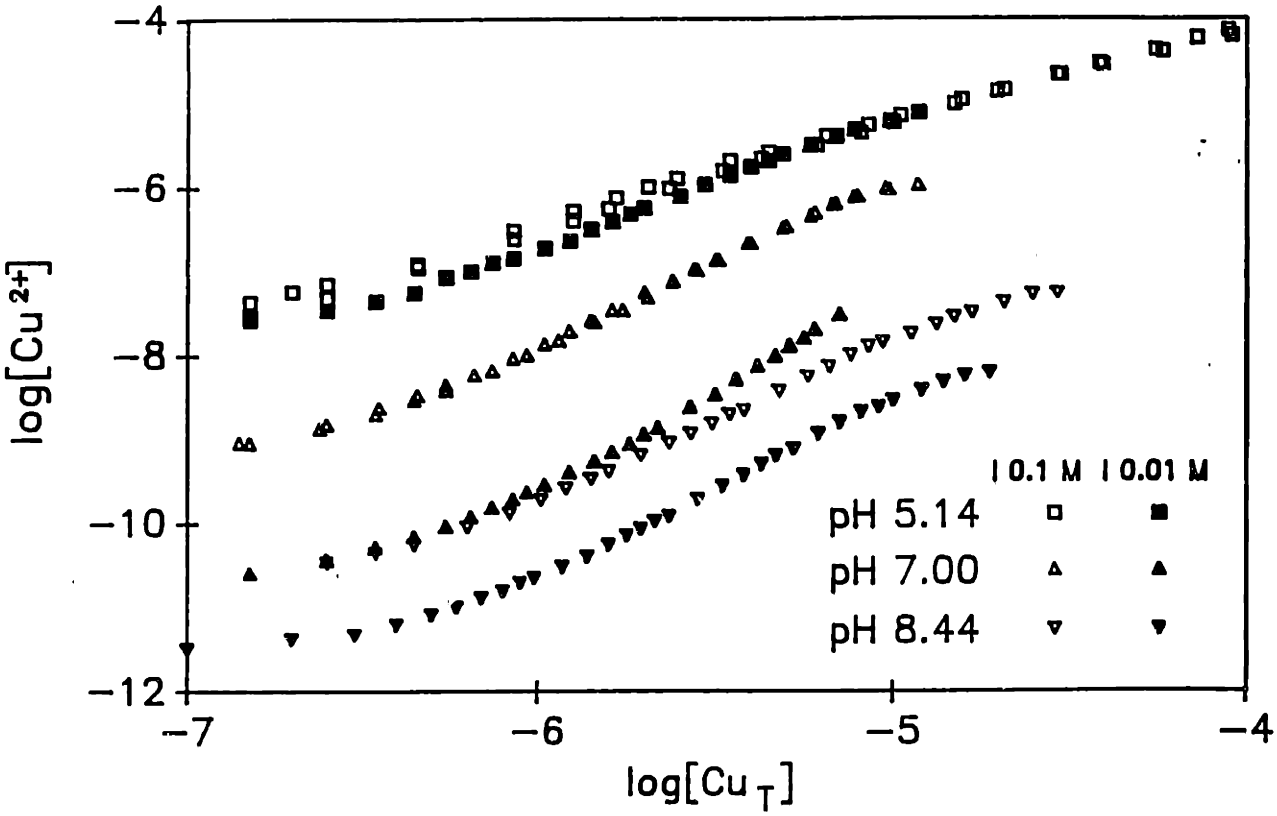

Figure 7. Lines show an attempt at fitting the data using one copper binding site and one size group (radius R = 15 Å, molecular weight = 5260 daltons), using equilibrium constants and total ligand concentrations shown in Table 2. An additional acidic (but not copper binding) site dominates the electrostatics. The solid lines and dotted lines represent model results for ionic strengths 0.01 M and 0.1 M respectively, at pH's 5.14, 7.00, and 8.44. The symbols represent the data shown in figure 6.

This and subsequent model fits use an impenetrable sphere model with the same size to charge density relationship as the one used in figure 3.

Figure 7

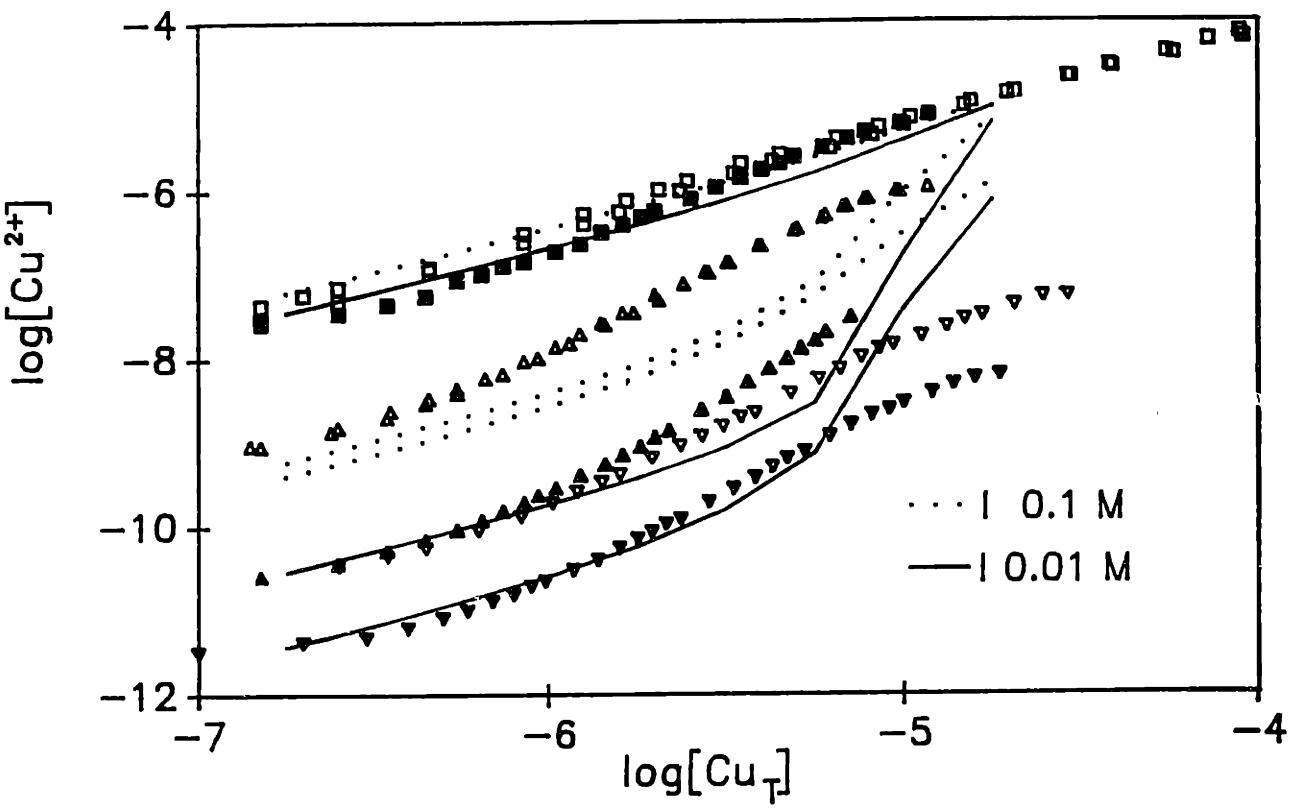

Figure 8. Ionic strength effect on a model pH titration, using the same model parameters as in figure 7. The total concentration of dissociated acidic sites in the solution, represented as "[A^-]", is given by $[OH^-]_{added} - [OH^-] + [H^+]$.

Figure 8

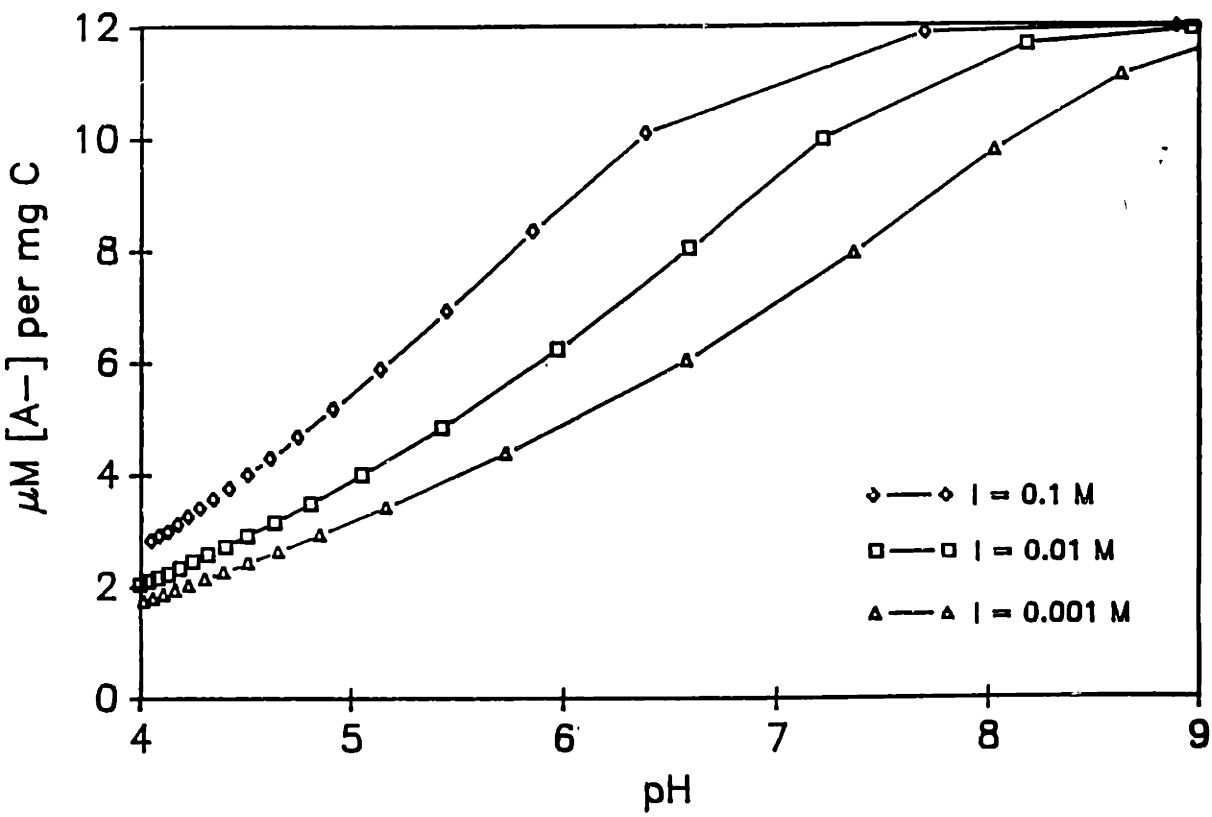

Figure 9. Model results using one copper binding site, one acidic site (see Table 2), and two size groups:

R = 7.7 Å, molecular weight = 711 daltons, 75 % by weight,

and R = 15 Å, molecular weight = 5260 daltons, 25 % by weight.

Solid lines and dotted lines represent model results for ionic strengths 0.01 M and 0.1 M respectively, at pH's 5.14, 7.00, and 8.44; symbols represent the data shown in figure 6.

Figure 9

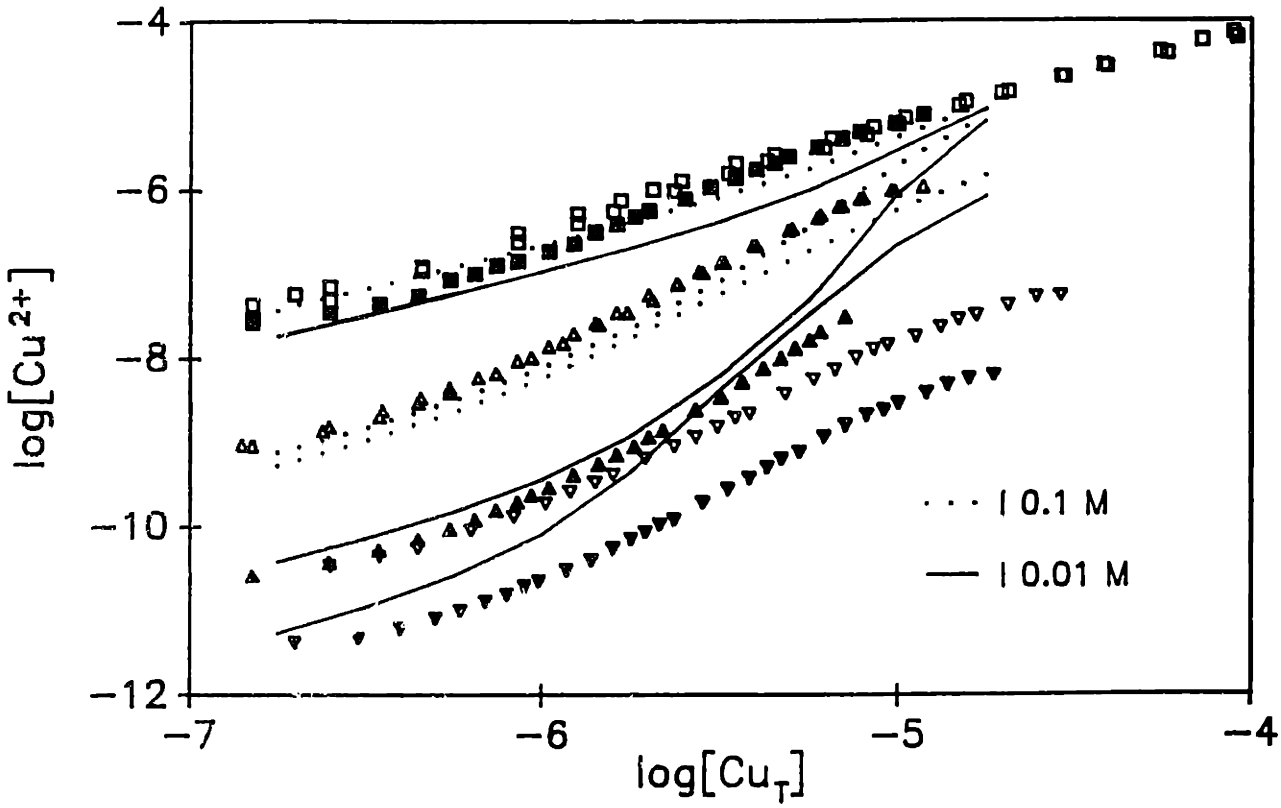

Figure 10. Ionic strength effects on a model pH titration using the same parameters as in figure 9.

Figure 10

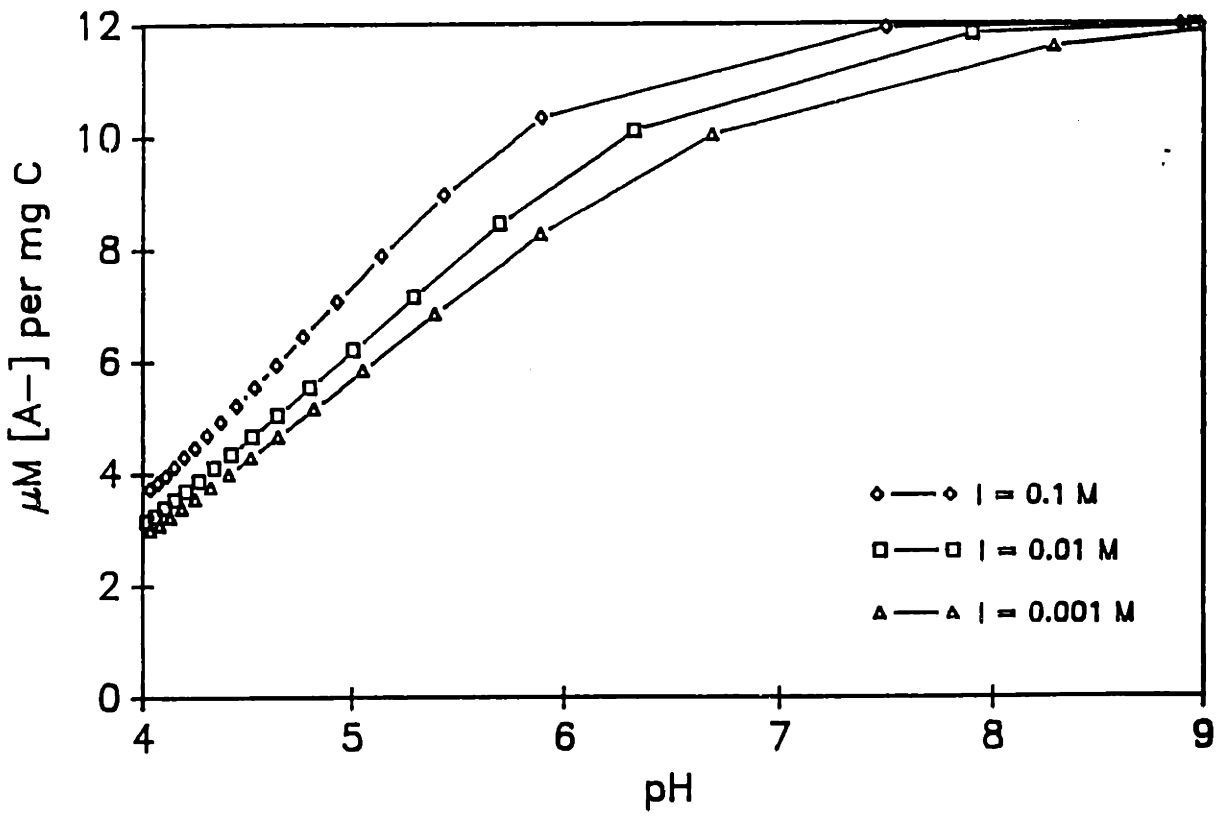

Figure 11. Model results using two copper binding sites, one acidic site (Table 2), and the same two size groups used in figure 9. Solid lines and dotted lines represent model results for ionic strengths 0.01 M and 0.1 M respectively, at pH's 5.14, 7.00, and 8.44; symbols represent the data shown in figure 6.

Figure 11

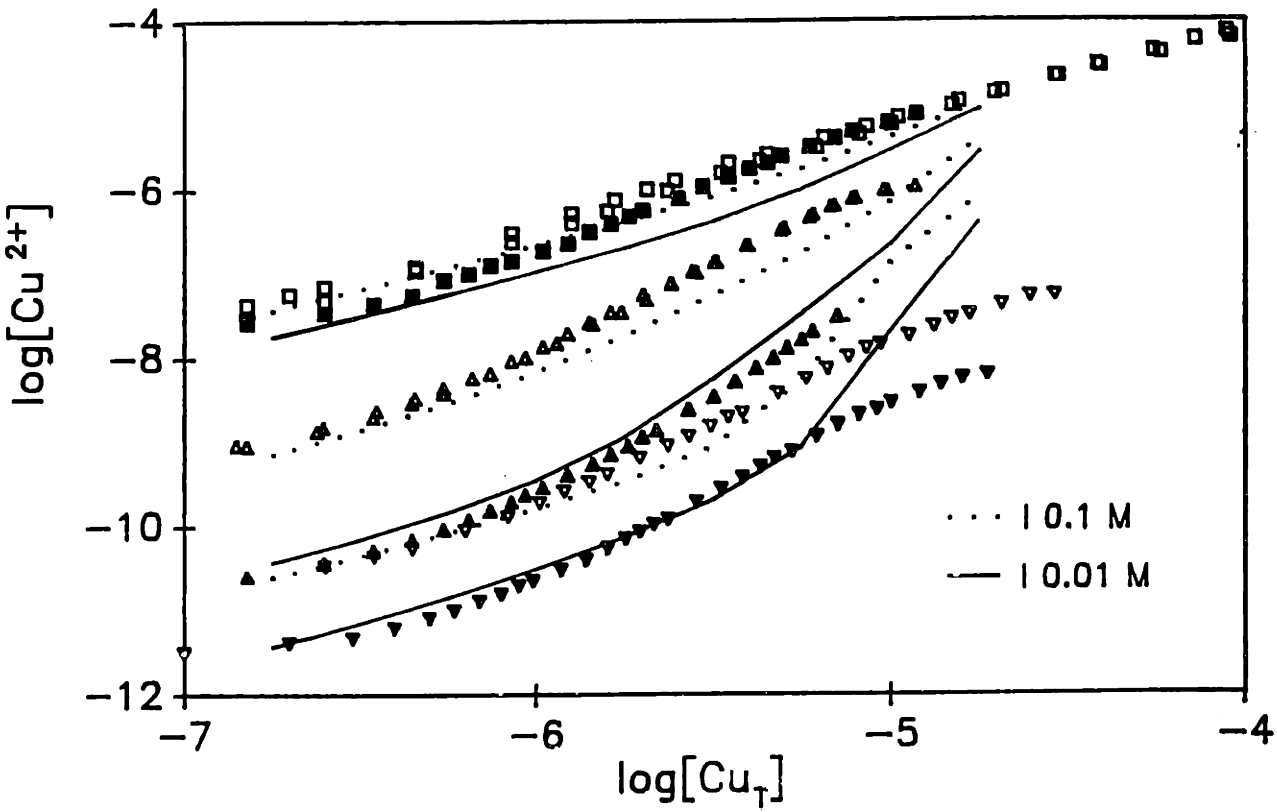

Figure 12. Ionic strength effects on a model pH titration using the same parameters as in figure 11.

Figure 12

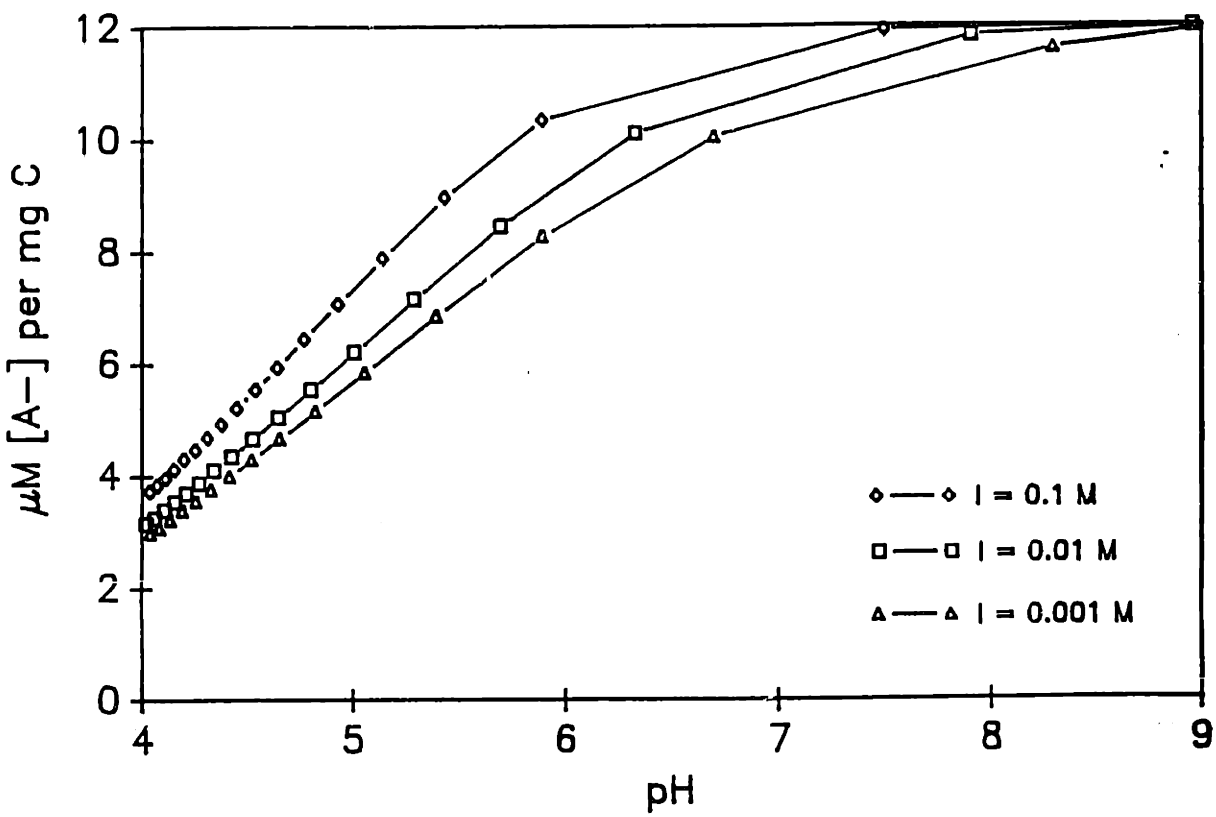

Appendix A

Although numerical solutions for the Poisson-Boltzmann equation of penetrable and impenetrable spheres have previously been derived (Wall and Berkowitz, 1957; Hermans and Overbeek, 1948), they are not of a convenient form for our purposes; we therefore chose to rely on our own computations.

Penetrable sphere

The spherical form of the Poisson-Boltzmann equation is:

$$\frac{2}{\bar{r}}\frac{d\bar{\Psi}}{d\bar{r}} + \frac{d^2\bar{\Psi}}{d\bar{r}^2} = -c_1\left(e^{-\bar{\Psi}} - e^{\bar{\Psi}}\right) + c_2 \qquad \text{A.1}$$

where $\Psi = e\Psi/kT$, $r = r/R$ (the distance from the center of the sphere r divided its radius R), and c_1 and c_2 correspond to $\rho_{\pm}$ and ρ_o in equation 10 of the text. The constant c_1 is given by:

$$c_1 = \frac{1000\ F\ R^2 I}{\varepsilon kT} \qquad \text{A.2}$$

where F is the Faraday constant, ε is the permittivity of water at 25°C, and i is the ionic strength in M. The constant c_2 is zero everywhere except within the humic phase, where:

$$c_2 = \left(\frac{R^2 e^2}{\varepsilon kT}\right)\left(\frac{Q}{4/3\pi R^3}\right) \qquad \text{A.3}$$

Q is the number of negative charges on the molecule.

To solve equation A.1, we used a second-order finite difference approximation, resulting in the equation

$$\frac{2}{\bar{r}}\left[\frac{\bar{\Psi}_{i+1} - \bar{\Psi}_{i-1}}{2\ \Delta\bar{r}}\right] + \left[\frac{\bar{\Psi}_{i+1} - 2\bar{\Psi}_i + \bar{\Psi}_{i-1}}{\Delta\bar{r}^2}\right] = -c_1\ [\exp(-\bar{\Psi}_i) - \exp(\bar{\Psi}_i)] + c_2 \qquad \text{A.4}$$

for all internal nodes Ψ_i ($1<i<n+1$). The total number of nodes is n+1; Δr is the spacing between nodes and $r = (i-1)\ \Delta r$. Because the potential should approach zero at large distances from the molecule, we specify the boundary condition

$$\bar{\Psi}_{n+1} = 0 \qquad \text{A.5}$$

where Ψ_{n+1} is the right boundary node. Since the potential $\Psi(r)$ decays more slowly at low ionic strengths, the distance to the right boundary node, $n\Delta r$, was adjusted with ionic strength to assure the validity of equation A.5. The other boundary condition (equation 12 in the text) results in the equation

$$\frac{2\ (\bar{\Psi}_2 - \bar{\Psi}_1)}{\Delta\bar{r}^2} = -c_1\ [\exp(-\bar{\Psi}_1) - \exp(\bar{\Psi}_1)] + c_2 \qquad \text{A.6}$$

for the left boundary node Ψ_1.

The resulting non-linear system of n equations in n unknowns (Ψ_1 to Ψ_n) was solved using the Newton-Raphson method and a modified Thomas algorithm, following the methods of Press *et al.*(1986).The integral in equation 18 of the text was estimated by the Riemann sum:

$$\Psi_{ave} = \frac{kT}{e}\ \bar{\Psi}_{ave} = \frac{kT}{e}\left[\sum_{i=1}^{\frac{1}{\Delta\bar{r}}+1} \bar{\Psi}_i\ [(\bar{r}+\Delta\bar{r})^3 - \bar{r}^3]\right] \qquad \text{A.7}$$

(a reasonable approximation since Δr was usually less than 0.01).

The calculations were carried out on an IBM AT compatible using Turbo PASCAL (see computer code 1).

Impenetrable Spheres

The finite difference approximation described above was also used for the impenetrable case, with several modifications (see computer code 2). The constant c_2 was zero everywhere and the boundary condition given by equation 11 of the text resulted in the expression

$$\frac{2\,(\bar{\Psi}_2 - \bar{\Psi}_1)}{\Delta\bar{r}^2} = -c_1\,[\exp(-\bar{\Psi}_1) - \exp(\bar{\Psi}_1)] + c_3\left(2 - \frac{2}{\Delta\bar{r}}\right) \qquad \text{A.8}$$

for the left boundary node, where

$$c_3 = \left(\frac{Q}{4\pi R}\right)\left(\frac{e^2}{\varepsilon kT}\right) \qquad \text{A.9}$$

The value of the surface potential Ψ_o used in equation 15 is given by $(kT/e)\Psi_1$.

Appendix B

This appendix addresses some of the fundamental thermodynamic issues behind the use of the Poisson-Boltzmann equation to calculate solution activity coefficients. In the main body of this paper, we have used the idea of a "local" activity of metal ion near the charged polyions, $\{\overline{M^{Z+}}\} = \lambda^Z \{M^{Z+}\}$, to derive expressions for the electrostatic effect on the apparent equilibrium constants of metal-polyion reactions. Although this is an intuitively pleasing mental construct, we would like to show here that the electrostatic factor λ can also be interpreted as a ratio of polyion activities. This more rigorous approach emphasizes our models' formal similarity to the Debye-Hückel model and also clarifies why the models diverge from Debye-Hückel at low ionic strengths.

Debye-Hückel activity coefficients for ions in electrolyte solutions are calculated from the work required to bring a solution ion from a hypothetical uncharged state to its charge Q, assuming that with each infinitesimal increase in charge dq the ions surrounding the ion of interest rearrange themselves in the resulting potential field according to the Poisson-Boltzmann equation. The work is calculated from the Poisson-Boltzmann potential at the surface of the central ion:

$$W_{el} = \int_0^{Qe} \Psi_o(q)\, dq \qquad \text{B.1}$$

Assuming that W_{el} is the only non-chemical contribution to the free energy of the system, and using the linear approximation to the Poisson-Boltzmann equation (which results in a Ψ_o that is a linear function of q),

$$\ln \gamma_Q = \frac{W_{el}}{kT} = \frac{Qe\Psi_o(Q)}{2} \qquad \text{B.2}$$

Since it takes a finite amount of work to charge the ion when no other ions are present in the solution, it is customary to subtract out this contribution to W_{el}, guaranteeing that $\ln \gamma_Q$ equals zero when the ionic strength is equal to zero.

One could also define the activity coefficients of larger charged ions using equation B.1:

$$\ln \gamma_Q = \frac{1}{kT}\int_0^{Qe} \Psi_o(q)\, dq \qquad \text{B.3}$$

for an impenetrable sphere, and

$$\ln \gamma_Q = \frac{1}{kT} \int_0^{Qe} \left(\int_0^R \frac{3r^2}{R^3} \Psi(r,q)\, dr \right) dq \qquad \text{B.4}$$

for a penetrable sphere, where the inner integral sums the work required to charge each sphereical shell of thickness dr over the total volume of the sphere (Tanford, 1961). Note that equation B.2 is no longer valid since the linear approximation is expected to fail when the charge density is large. When a chemical reaction between the polyion and a small ion of charge Z is considered, it is the ratio of polyion activity coefficients γ_{Q+z}/γ_Q that will appear as the correction to K_{int} in the equilibrium expression, resulting in an "effective" activity coefficient

$$\gamma_{eff} = \ln \frac{\gamma_{Q+z}}{\gamma_Q} = \ln \gamma_{Q+z} - \ln \gamma_Q$$

$$= \frac{1}{kT}\int_{Qe}^{(Q+z)e} \Psi_o(q)\, dq \qquad \text{impenetrable sphere} \qquad \text{B.5}$$

$$= \frac{1}{kT} \int_{Qe}^{(Q+z)e} \left(\int_0^R \frac{3r^2}{R^3} \Psi(r,q)\, dr \right) dq \qquad \text{penetrable sphere} \qquad \text{B.6}$$

If Q is much larger than Z, Ψ_0 and $\Psi(r,Q)$ are approximately equal to $\Psi_0(Q+Z)$ and $\Psi(r, Q+Z)$ respectively, so that

$$\ln \gamma_{eff} = \frac{Ze}{kT}\Psi_o(Qe) \qquad \text{impenetrable sphere} \qquad B.7$$

$$= \frac{Ze}{kT}\int_0^R \frac{3r^2}{R^3}\Psi(r,Q)\,dr \qquad \text{penetrable sphere} \qquad B.8$$

Thus γ_{eff} equals λ as defined by equations 17 and 18 in the text as long as the charge of the polyion does not come close to being neutralized by the reaction..

The difference between this formulation and the Debye-Hückel model is that there is no easy way to define an activity coefficient that approaches 1 in the limit of zero ionic strength. In the non-linear formulation of the Poisson-Boltzmann equation, Ψ_0 does not approach a finite value as the ionic strength approaches zero, even though the work required to charge the sphere in the absence of counterions is finite. As was mentioned in the modeling section of the text, this poses a difficulty when one attempts to compare literature constants for which the reference state is zero ionic strength with intrinsic constants in the context of a polyion model, for which the reference state is zero potential (high ionic strength). Although the Debye-Hückel model and the sphere models presented in this paper are products of the same thermodynamical foundations, the issues surrounding this discrepancy in possible reference states remain to be resolved.

Computer program 1

```
program psicalc (input, output);

const
     RO      = 20e-10 ;     {outer radius in m}
     R1      = 1e-10;       {inner radius in m}
     Q       = 50;          {number of charges in humic phase}
     I       = 0.1 ;        {ionic strength in moles/l}
     n       = 100 ;         {number of nodes in approximation}
     n1      = 101 ;         {n + 1}
     length  = 5   ;         {range from r=R1 to r=length*(RO-R1)}
     alph    = 1.00  ;      {proportion of solvated penetrable phase volume}
     itmax   = 25    ;      {number of iterations before stopping}
     tolrx   = 0.01  ;       {values for convergence test}
     tolrf   = 0.0001  ;
     Ka      = 1e-4;         {Ka of acidic site}
     H       = 1e-12;         {hydrogen ion concentration}
     version = 'pH - pKa = 8';
     e       = 1.602e-19;   {elementary charge in c}
     epsilon = 6.954e-10;   {permittivity of water at 25 C}
     T       = 298;         {temperature in K}
     k       = 1.381e-23;   {Boltzman's constant}
     F       = 96500   ;    {Faraday's constant}
     pi      = 3.14159  ;
     NA      = 6.023e23;    {Avogadro's number}

type
    glnarray = array[1..n1] of real;
    glnbyn   = array[1..n,1..5] of real;
    glindx   = array[1..n] of integer;

var
    dV, a, b, r, kappa, Qave, psiave, lambdave, deltar, erx, erf : real;
    x, psi, beta : glnarray;
    z,j: integer;
    datafile, prnt: text;
    filename: string;
    answer: char;
    alpha : glnbyn;

function dissacid(ps : real) : real;
     begin

dissacid := 1/(1+exp(-ps)*H/Ka);
     end;

function derivdiss(ps : real) : real;
     begin
     derivdiss := sqr(dissacid(ps)) * exp(-ps) * H/Ka;
     end;

function cube(z : real) : real;
begin
     cube := z*z*z;
end;procedure usrfun(x: glnarray; n: integer; VAR beta: glnarray);
var
   i,j : integer;


begin
     for i := 1 to n do
     begin                          {initialize alpha matrix}
          for j := 1 to 5 do
               alpha[i,j] := 0;
     end;

     beta[1] := -1*(-2*x[1]/sqr(deltar) + a*(exp(-1*x[1])-exp(x[1]))
```

```
                + 2*x[2]/sqr(deltar) - b*dissacid(x[1]));
    alpha[1,3] := -2/sqr(deltar) - a*(exp(-1*x[1])+exp(x[1]))
                  -b*derivdiss(x[1]);
    alpha[1,4] := 2/sqr(deltar);
    for i := 2 to n-1 do
        begin
            r := R1/R0 + (i-1)*deltar;
            beta[i] := -1*((-1/deltar + r/sqr(deltar))*x[i-1]
                  - 2*r*x[i]/sqr(deltar) + a*r*(exp(-1*x[i])-exp(x[i]))
                  + (1/deltar + r/sqr(deltar))*x[i+1] - b*r*dissacid(x[i]));
            alpha[i,2] := -1/deltar + r/sqr(deltar);
            alpha[i,3] := -2*r/sqr(deltar) - a*r*(exp(-1*x[i])+exp(x[i]))
                          -b*r*derivdiss(x[i]);
            alpha[i,4] := 1/deltar + r/sqr(deltar);
            if i = ((n div length) +1) then
               begin
                    beta[i] := -1/cube(deltar) * ( x[i-2] - 2*x[i-1]
                                  + 2*x[i+1] - x[i+2]) - 1/deltar*b*dissacid(x
[i]);
                    alpha[i,1] := 1/cube(deltar);
                    alpha[i,2] := -2/cube(deltar);
                    alpha[i,3] :=  1/deltar*b*derivdiss(x[i]);
                    alpha[i,4] :=  2/cube(deltar);
                    alpha[i,5] := -1/cube(deltar);
               end;

            if i > ((n div length) +1) then
               beta[i] := beta[i] - b*r*dissacid(x[i]);
               alpha[i,3] := alpha[i,3] + b*r*derivdiss(x[i]);
         end;

    r := R1/R0 + (n-1)*deltar;
    beta[n]  := -1*((-1/deltar + r/sqr(deltar))*x[n-1] -2*r*x[n]/sqr(deltar)
                + a*r*(exp(-x[n])-exp(x[n])));
    alpha[n,2] := -1/deltar + r/sqr(deltar);
    alpha[n,3] := -2*r/sqr(deltar) - a*r*(exp(-1*x[n])+exp(x[n]));
    end;

procedure thomas(d: glnarray);

{expanded Thomas algorithm -- banded matrix solver}

VAR
   i : integer;
   quotient : real;

BEGIN
{Gaussian elimination}
    alpha[1,1] := 0; alpha[1,2] := 0; alpha[2,1] := 0; alpha[n-1,5] := 0;
    alpha[n,4] := 0; alpha[n,5] := 0;
    alpha[1,4] := alpha[1,4]/alpha[1,3]; alpha[1,5] := alpha[1,5]/alpha[1,3];
    d[1] := d[1]/alpha[1,3];
    alpha[1,3] := 1;
         for i := 2 to n do
         begin
              quotient := alpha[i,3] - alpha[i,1]*alpha[i-2,5] -
                  alpha[i-1,4]*(alpha[i,2] - alpha[i,1]*alpha[i-2,4]);
              d[i] := (d[i]-alpha[i,1]*d[i-2]-(alpha[i,2] - alpha[i,1]*
                  alpha[i-2,4])*d[i-1])/quotient;
              alpha[i,1] := 0;
              alpha[i,2] := 0;
              alpha[i,3] := 1;
              alpha[i,4] := (alpha[i,4] - (alpha[i,2] - alpha[i,1]*
                  alpha[i-2,4])*alpha[i-1,5])/quotient;
              alpha[i,5] := alpha[i,5]/quotient;
         end;
```

```
{backsubstitution}
     beta[n] := d[n];
     beta[n-1] := d[n-1] - alpha[n-1,4]*beta[n];
     for i := n-1 downto 1 do
          beta[i] := d[i] - alpha[i,4]*beta[i+1] - alpha[i,5]*beta[i+2];
end;

procedure printoutput;

var
     j: integer;

begin
     assign (prnt,'PRN');
     rewrite(prnt);
     writeln(prnt, version);
     writeln(prnt,'R1 = ',R1*1e10:5:1,' A.   RO = ',RO*1e10:5:1,'A.');
     writeln(prnt,'Q  = ',Q:5,'.     I.S. =',I:8:5,'M.');
     writeln(prnt,'Saved as filename ',filename,'.   alpha = ',alph:5:2);
     writeln(prnt,'errx = ',erx:8:5,'.  errf = ',erf:8:5,'.');
     j := 1;
     writeln(prnt,'  Radius (A)       psi.corr     psi.Tanford');
     repeat
     writeln(prnt,(R1 + RO*(j-1)*deltar)*1e10:10:3,'     ',
                  x[j]:10:3,'     ',psi[j]:10:3);
     j := j + 1;
     until j>(n+1);
     close (prnt);
end;


PROCEDURE mnewt(ntrial: integer; VAR x: glnarray; n: integer;
      tolx,tolf: real);

LABEL 99;
VAR
   k,i: integer;
   errx,errf,d: real;
   indx: glindx;
BEGIN
   FOR  k := 1 to ntrial DO BEGIN
      writeln('iteration ',k);
      usrfun(x,n,beta);
      errf := 0.0;
      FOR i := 1 to n DO errf := errf+abs(beta[i]);
      IF (errf <= tolf) THEN
         begin
         writeln('errf <= tolf after ',k,' iterations.');
         GOTO 99;
         end;
      thomas(beta);
      errx := 0.0;
      FOR i := 1 to n DO BEGIN
         errx := errx+abs(beta[i]);
         x[i] := x[i]+beta[i]
      END;
      writeln('errx = ',errx:12:5,'.      errf = ',errf:12:5,'.');
      erx := errx; erf := errf;
      IF (errx <= tolx) THEN
      begin
      writeln('errx <= tolx after ',k,' iterations.');
      GOTO 99;
      end;

   END;
   writeln('stopped after ',ntrial,' iterations.');
```

```
99:writeln('errx = ',errx:8:5,'.  errf = ',errf:8:5,'.');

   END;



function psiII(r : real) : real;
var
   f1,f2,f3,f4 : real;

begin
   f1 := (1+ alph*kappa*R1) / (1-alph*kappa*R1);
   f2 := f1*exp(alph*kappa*(r+RO-2*R1))-exp(alph*kappa*(RO-r));
   f3 := (1+alph)*f1*exp(2*alph*kappa*(RO-R1)) - 1 + alph;
   f4 := 3*Q*e*(1+kappa*RO)/(cube(kappa)*4*pi*epsilon*sqr(alph)
         *(cube(RO)-cube(R1)));
   psiII := -1* f4 * ((kappa/(1+kappa*RO)) - f2/(r*f3));
end;

function psiIII(r : real) : real;
begin
     psiIII := RO * psiII(RO) * exp(-1*kappa*(r-RO)) / r;
end;



begin
     write('printer output ? ');
     readln(answer);
     write('filename = ');
     readln(filename);
     assign(datafile,filename);
     rewrite(datafile);
     a := sqr(RO)*e*1000*F*I/(epsilon*k*T);
     b := sqr(RO)/(epsilon*k*T*4/3*pi)*sqr(e)*Q/(cube(RO)-cube(R1));
     kappa := sqrt(2*sqr(e)*NA*1000*I/(epsilon*k*T));
     deltar := length/n*(RO-R1)/RO;

     {set up initial guess:  Tanford model...}

     for j := 1 to n+1 do
     begin
     r := R1 + RO*(j-1)*deltar;
     if j< ((n div length) + 1)
        then x[j] := e*psiII(r)/(k*T)
        else x[j] := e*psiIII(r)/(k*T);
     psi[j] := x[j]; x[j] := 0;
     end;

     {solve for corrected model}

     mnewt(itmax,x,n,tolrx,tolrf);
     x[n+1] := 0; {boundary condition on right side}
     Qave := 0; psiave := 0; lambdave := 0;
     {print results}

     if answer = 'y' then printoutput;
     writeln('R1 = ',R1*1e10:5:1,' A.   RO = ',RO*1e10:5:1,'A.');
     writeln('Q  = ',Q:5,'.     I.S. =',I:8:5,'M.');
     writeln('Saved as filename ',filename,'.   alpha = ',alph:5:2);
     j := 1;
     writeln('  Radius (A)       psi.corr      psi.Tanford');
```

```
    repeat
        writeln((R1 + RO*(j-1)*deltar)*1e10:10:3,'    ',x[j]:10:3,'     '
                ,psi[j]:10:3);
        for z := j to j+9 do
            begin
                writeln(datafile,(R1 + RO*(z-1)*deltar)*1e10:10:3,',',
                    (R1 + RO*(z-1)*deltar)/RO:10:3,',',x[z]:10:3,',',
                    psi[z]:10:3);
                if z < (n div length) + 1 then
                    begin
                    r := R1/RO + (z-1)*deltar;
                    dV := (cube(r+deltar) - cube(r))/(1-cube(R1/RO));
                    Qave := Qave + dV*dissacid(x[z]);
                    psiave := psiave + dV*x[z];
                    lambdave := lambdave + dV*exp(-x[z]);
                    end;
            end;
        j := j + 10;
    until j>(n+1);

    writeln('average charge = ',Qave*Q:6:2,' .');
    writeln('average psi = ',psiave:5:3,' .');
    writeln('average lambda = ',lambdave:5:1,' .');

    writeln(datafile,'average charge = ',Qave*Q:6:2,' .');
    writeln(datafile,'average psi = ',psiave:5:3,' .');
    writeln(datafile,'average lambda = ',lambdave:5:1,' .');

    close(datafile);

end.
```

Computer program 2

```
program psicalc (input, output);

const
     RO      = 7.7E-10 ;    {outer radius in m}
     Qmax    = 16;          {number of charges in humic phase}
     maxpoints = 25;
     I       = 0.001;       {ionic strength in moles/l}
     n       = 500 ;        {number of nodes in approximation}
     n1      = 501 ;        {n + 1}
     length  = 300e-10  ; {distance from edge of molecule to "R-infinity"}
     itmax   = 100   ;      {number of iterations before stopping}
     tolrx   = 0.001  ;     {values for convergence test}
     tolrf   = 0.0001  ;
     Ka      = 1e-4;        {Ka of acidic site}
     H       = 1e-12;       {hydrogen ion concentration}
     version = 'pH - pKa = 8';
     e       = 1.602e-19;  {elementary charge in c}
     epsilon = 6.954e-10;  {permittivity of water at 25 C}
     T       = 298;        {temperature in K}
     k       = 1.381e-23;  {Boltzman's constant}
     F       = 96500   ;   {Faraday's constant}
     pi      = 3.14159  ;
     NA      = 6.023e23;   {Avogadro's number}

type
    glnarray = array[1..n1] of real;
    glnbyn   = array[1..n,1..3] of real;
    glindx   = array[1..n] of integer;

var
    sigma, Q, dV, a, b, r, kappa, deltar, erx, erf : real;
    x, psi, beta : glnarray;
    z,j,point: integer;
    datafile, prnt: text;
    filename: string;
    answer: char;
    alpha : glnbyn;


procedure usrfun(x: glnarray; n: integer; VAR beta: glnarray);
var
   i,j : integer;


begin
     for i := 1 to n do
     begin                              {initialize alpha matrix}
          for j := 1 to 3 do
               alpha[i,j] := 0;
     end;

     beta[1] := -1*(-2*x[1]/sqr(deltar) + a*(exp(-1*x[1])-exp(x[1]))
                + 2*x[2]/sqr(deltar) - b*(2 - 2/deltar));
     alpha[1,2] := -2/sqr(deltar) - a*(exp(-1*x[1])+exp(x[1]));
     alpha[1,3] := 2/sqr(deltar);
     for i := 2 to n-1 do
         begin
              r := 1 + (i-1)*deltar;
              beta[i] := -1*((-1/deltar + r/sqr(deltar))*x[i-1]
                    - 2*r*x[i]/sqr(deltar) + a*r*(exp(-1*x[i])-exp(x[i]))
                    + (1/deltar + r/sqr(deltar))*x[i+1]);
              alpha[i,1] := -1/deltar + r/sqr(deltar);
              alpha[i,2] := -2*r/sqr(deltar) - a*r*(exp(-1*x[i])+exp(x[i]));
              alpha[i,3] := 1/deltar + r/sqr(deltar);

         end;
```

```
      r := 1 + (n-1)*deltar;
      beta[n]  := -1*((-1/deltar + r/sqr(deltar))*x[n-1] -2*r*x[n]/sqr(deltar)
                  + a*r*(exp(-x[n])-exp(x[n])));
      alpha[n,1] := -1/deltar + r/sqr(deltar);
      alpha[n,2] := -2*r/sqr(deltar) - a*r*(exp(-1*x[n])+exp(x[n]));
      end;

procedure thomas(d: glnarray);

{Thomas algorithm -- banded matrix solver}

VAR
   i : integer;
   quotient : real;

BEGIN
{Gaussian elimination}
      alpha[1,1] := 0; alpha[n,3] := 0;
      alpha[1,3] := alpha[1,3]/alpha[1,2];
      d[1] := d[1] / alpha[1,2];
      alpha[1,2] := 1;
      for i := 2 to n do
          begin
               quotient := alpha[i,2] - alpha[i,1]*alpha[i-1,3];
               d[i] := (d[i]-alpha[i,1]*d[i-1])/quotient;
               alpha[i,1] := 0;
               alpha[i,2] := 1;
               alpha[i,3] := alpha[i,3]/quotient;
          end;
{backsubstitution}
      beta[n] := d[n];
      for i := n-1 downto 1 do
           beta[i] := d[i] - alpha[i,3]*beta[i+1];
end;

procedure printoutput;

var
      j: integer;

begin
      assign (prnt,'PRN');
      rewrite(prnt);
      writeln(prnt, version);
      writeln(prnt,'RO = ',RO*1e10:5:1,'A.');
      writeln(prnt,'Q  = ',Q:5,'.     I.S. =',I:8:5,'M.');
      writeln(prnt,'Saved as filename ',filename,'.');
      writeln(prnt,'errx = ',erx:8:5,'.  errf = ',erf:8:5,'.');
      j := 1;
      writeln(prnt,'  Radius (A)       psi.corr     psi.Tanford');
      repeat
      writeln(prnt,(RO + RO*(j-1)*deltar)*1e10:10:3,'    ',
                   x[j]:10:3,'     ',psi[j]:10:3);
      j := j + 1;
      until j>(n+1);
      close (prnt);
end;


PROCEDURE mnewt(ntrial: integer; VAR x: glnarray; n: integer;
       tolx,tolf: real);

LABEL 99;
VAR
   k,i: integer;
```

```
   errx,errf,d: real;
   indx: glindx;
BEGIN
   FOR  k := 1 to ntrial DO BEGIN
      write(k);
      usrfun(x,n,beta);
      errf := 0.0;
      FOR i := 1 to n DO errf := errf+abs(beta[i]);
      IF (errf <= tolf) THEN
         GOTO 99;
      thomas(beta);
      errx := 0.0;
      FOR i := 1 to n DO BEGIN
         errx := errx+abs(beta[i]);
         x[i] := x[i]+beta[i]
      END;
      erx := errx; erf := errf;
      IF (errx <= tolx) THEN
      GOTO 99;

   END;
   writeln('stopped after ',ntrial,' iterations.');

99:writeln;
   END;


function cube(z : real) : real;
begin
     cube := z*z*z;
end;




begin
     write('printer output ? ');
     readln(answer);
     write('filename = ');
     readln(filename);
     assign(datafile,filename);
     rewrite(datafile);
     for j := 1 to n+1 do
         x[j] := 0;

  for point := 0 to maxpoints do
     begin
     Q := point * Qmax /maxpoints;
     a := sqr(RO)*e*1000*F*I/(epsilon*k*T);
     b := Q/RO*7.135e-10;
     kappa := sqrt(2*sqr(e)*NA*1000*I/(epsilon*k*T));
     deltar := length/n/RO;
     sigma := Q*e/(4*pi*sqr(RO))*100; {surface charge density in microC/cm^2}

     {solve for corrected model}

     mnewt(itmax,x,n,tolrx,tolrf);
     x[n+1] := 0; {boundary condition on right side}

     {print results}

     if answer = 'y' then printoutput;

     writeln(Q:6:3,sigma:10:4,x[1]/2.303:10:3);
```

```
        write(datafile,Q:6:3,',',sigma:6:4,',',x[1]/2.303:10:3,',');
        end;

        close(datafile);

end.
```